

Extended optical theorem in isotropic solids and its application to the elastic radiation force

J. P. Leão-Neto,¹ J. H. Lopes,² and G. T. Silva^{1, a)}

¹⁾*Physical Acoustics Group, Instituto de Física, Universidade Federal de Alagoas, Maceió, AL 57072-970, Brazil*

²⁾*Grupo de Física da Matéria Condensada, Núcleo de Ciências Exatas, Universidade Federal de Alagoas, Arapiraca, AL 57309-005, Brazil*

(Dated: Ver. 20)

The optical theorem is an important tool for scattering analysis in acoustics, electromagnetism, and quantum mechanics. We derive an extended version of the optical theorem for the scattering of elastic waves by a spherical inclusion embedded in a linear elastic solid using a vector spherical harmonics representation of the waves. The sphere can be a rigid, empty cavity, elastic, viscoelastic, or layered material. The theorem expresses the extinction cross-section, i.e. the time-averaged power extracted from the incoming beam per its intensity, regarding the partial-wave expansion coefficients of the incident and scattered waves. We establish the optical theorem for a longitudinal spherically focused beam scattered by a sphere. Moreover, we use the optical theorem formalism to obtain the radiation force exerted on an inclusion by an incident plane wave and focused beam. Considering an iron sphere embedded in an aluminum matrix, we compute the scattering and elastic radiation force efficiencies. In addition, the elastic radiation force is obtained on a stainless steel sphere embedded in a tissue-like medium (soft solid). Remarkably, we find a relative difference of up to 98% between our findings and previous lossless liquid models. Regarding some applications, the obtained results have a direct impact on ultrasound-based elastography techniques, ultrasonic nondestructive testing, as well as implantable devices activated by ultrasound.

PACS numbers: 43.25.Qp, 43.40.Fz, 43.35.Cg

I. INTRODUCTION

Mechanical, electromagnetic, and quantum-mechanical wave scattering share some remarkable universal features. A striking common characteristic among these fields is the optical theorem. The original idea behind it was to relate the optical index of refraction of a medium to what has been extinct in the scattering process¹. For a traveling plane wave, the optical theorem states that the extinction cross-section, i.e. the time-averaged power extracted from the incident wave by scattering and absorption per incident intensity, is tantamount the forward scattering function. The theorem was initially stated for electromagnetic waves². In quantum-mechanics, it was derived by Feenberg³. The optical theorem was also established for a plane electromagnetic^{4,5}, plane sound wave in an ideal fluid⁵, and plane elastic waves in solids⁶⁻¹⁰. A generalized form of the optical theorem was proposed in the electron diffraction theory using reciprocity relations¹¹ and in the acoustic scattering by objects with inversion symmetry^{12,13}. Furthermore, the generalized theorem was obtained for waves in a stratified medium¹⁴, surface waves^{15,16}, and Raman scattering by fractal clusters¹⁷.

It has been noticed that the ordinary optical theorem established for plane waves has some limitations. It cannot be applied to beams with some transverse amplitude roll-off such as Gaussian beams¹⁸. An extension of the optical theorem for nonplane wave scattering by a radially symmetric potential in quantum mechanics was presented in Ref.¹⁹. In this case, both incident and scattered eigenstates are expanded in spherical function bases, allowing the extinction cross-section be expressed in terms of the expansion coefficients. Another extended optical theorem was derived for the on-axis scattering of a non-diffracting acoustic beam (such as Bessel beams) propagating in an ideal fluid²⁰. This result was subsequently generalized for a scalar beam with arbitrary wavefront²¹. This problem has outstanding similarity with the inelastic scattering of quantum beams by a radial symmetric potential²². Extended optical theorems using the cylindrical wave decomposition has also been established for both acoustic^{23,24} and electromagnetic²⁵ waves.

^{a)}Electronic mail: glauber@pq.cnpq.br

As noted by Newton¹, the optical theorem accounted for dispersion of light propagating in a material. A description of x-rays dispersion was also provided based on similar ideas²⁶. It also served as the foundation of the connection between dispersion relation and causality²⁷. A wide variety of applications of the optical theorem includes phase shift estimation from measurements of the differential scattering cross-section in quantum mechanics²⁸, evaluation of cracks in elastic solids^{29,30}, diffraction tomography³¹, analysis of attenuation effects from scatterers³², Green's function reconstruction in inhomogeneous elastic solid medium³³, seismic interferometry³⁴, and calculation of energy loss in solids with dislocation³⁵, to name a few. In ultrasonic nondestructive testing (NDT)³⁶, an ultrasound wave is employed to investigate solid structures with inclusions, dislocation, and microcracks³⁷.

Motivated by the wide range of applications that the optical theorem may bring to elastodynamics and NDT, we developed the extended formalism applicable to any longitudinal or shear ultrasound beam of an arbitrary wavefront. Also, we apply the optical theorem framework to derive the mean force exerted on the inclusion in a solid matrix by elastic waves. In lossless fluids, this force, known as the acoustic radiation force, has been theoretically analyzed in Refs.³⁸⁻⁴⁵. In solids, we refer to it as *the elastic radiation force*. This force plays a key role in some elastography methods⁴⁶⁻⁴⁹. It is also related to the ultrasound-activation mechanism for implanted devices⁵⁰. Moreover, the displacement induced by the elastic radiation force on a particle embedded in a viscoelastic gel has been experimentally measured^{51,52}.

With the developed formalism, we revisit the scattering of longitudinal and shear plane waves by a spherical inclusion. We derive the optical theorem for the scattering of a longitudinal spherically focused beam by an on-focus sphere. We numerically compute the extinction and radiation force efficiencies for the scattering of the beams mentioned above. The incident waves are scattered by an iron sphere embedded in an aluminum matrix. The role of mode conversion in scattering is featured. Additionally, we consider a stainless steel sphere in a tissue-like medium (soft solid). The obtained radiation force considerably deviates from that computed based on the previous lossless liquid model for the medium³⁹. A 98%-relative difference is found between our findings and previous models. Thus, estimating the radiation force in soft solids assuming a liquid medium may lead to an enormous error. This work was partially presented in the 5th Joint Meeting of the Acoustical Society of America and Acoustical Society of Japan, Honolulu, Hawaii, 2016.

II. THEORY

A. Wave propagation and scattering

Consider an unbounded medium composed of an isotropic elastic solid with density ρ_0 . The displacement vector of a point at position vector \mathbf{r} is denoted by \mathbf{u} . The stress induced by small perturbation in the medium is based on the Hooke's law,⁵³

$$\boldsymbol{\sigma} = K_0 (\nabla \cdot \mathbf{u}) \mathbf{I} + \mu_0 (\nabla \mathbf{u} + \nabla \mathbf{u}^T), \quad (1)$$

where the constants K_0 and μ_0 are, respectively, the bulk and shear modulus, \mathbf{I} is the second-rank unit tensor, $\nabla \mathbf{u}$ is a second-rank tensor, and the superscript T denotes the transpose operation. The conservation of linear momentum requires

$$\rho_0 \partial_t^2 \mathbf{u} = \nabla \cdot \boldsymbol{\sigma}. \quad (2)$$

Here, we are using the shorthand notation $\partial_t = \partial/\partial t$. Substituting Eq. (1) into this equation yields

$$\rho_0 \partial_t^2 \mathbf{u} = (K_0 + \mu_0) \nabla (\nabla \cdot \mathbf{u}) + \mu_0 \nabla^2 \mathbf{u}. \quad (3)$$

This is the wave equation supporting longitudinal (L) and shear (S) waves. By employing the identity $\nabla^2 \mathbf{u} = \nabla (\nabla \cdot \mathbf{u}) - \nabla \times \nabla \times \mathbf{u}$, we obtain

$$\partial_t^2 \mathbf{u} = c_L^2 \nabla (\nabla \cdot \mathbf{u}) - c_S^2 \nabla \times \nabla \times \mathbf{u}, \quad (4)$$

where the longitudinal and shear speed of sound are, respectively,

$$c_L = \sqrt{\frac{K_0 + 2\mu_0}{\rho_0}}, \quad c_S = \sqrt{\frac{\mu_0}{\rho_0}}. \quad (5)$$

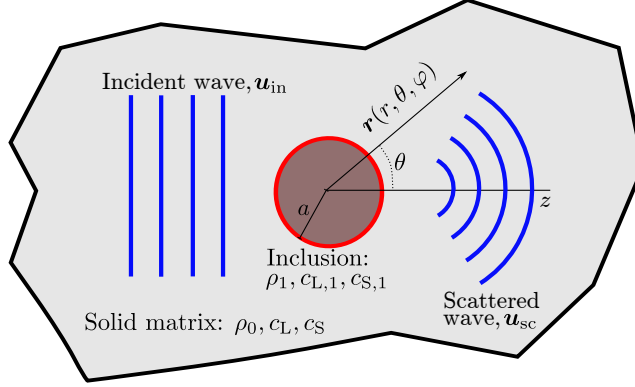


FIG. 1. (Color online) The sketch of the scattering problem. An arbitrary incident wave denoted by blue vertical bars is scattered by a spherical inclusion of radius a , density ρ_1 , longitudinal $c_{L,1}$ and shear $c_{S,1}$ speed of sound. The sphere is embedded in a solid matrix of density ρ_0 , longitudinal c_L and shear c_S speed of sound. The scattered waves are depicted by blue arches. The axial z -direction and position vector in spherical coordinates (r, θ, φ) are illustrated.

Note that the longitudinal speed of sound is larger than its shear counterpart, $c_L > c_S$.

Assume that a time-harmonic displacement of angular frequency ω is induced in the solid. Using the Helmholtz decomposition theorem⁵⁴, we can express the displacement amplitude vector as

$$\mathbf{u} = \left[\mathbf{u}^{(L)} + \mathbf{u}^{(S)} \right] e^{-i\omega t}, \quad (6)$$

where ‘ i ’ is the imaginary-unit, $\mathbf{u}^{(L)}$ (longitudinal component) is irrotational $\nabla \times \mathbf{u}^{(L)} = 0$, and $\mathbf{u}^{(S)}$ (shear component) is divergenceless $\nabla \cdot \mathbf{u}^{(S)} = 0$.

Hereafter, we consider the longitudinal $\mathbf{u}^{(L)}$ and shear $\mathbf{u}^{(S)}$ displacements as normalized quantities to the displacement magnitude u_0 . Inserting Eq. (6) into Eq. (4), we find the vector Helmholtz equations,

$$(\nabla^2 + k_L^2) \mathbf{u}^{(L)} = 0, \quad (7a)$$

$$(\nabla^2 + k_S^2) \mathbf{u}^{(S)} = 0, \quad (7b)$$

where $k_L = \omega/c_L$ and $k_S = \omega/c_S$ are the longitudinal and shear wavenumbers, respectively.

In the presence of an inclusion, both incident longitudinal and shear waves will be scattered. In Fig. 1 we illustrate the scattering problem for a sphere of radius a and density ρ_1 embedded in an elastic solid.

The longitudinal and shear speed of sound of the sphere are denoted by $c_{L,1}$ and $c_{S,1}$, respectively. For convenience, we adopt spherical coordinates (r, θ, φ) , where r is the radial distance, θ and φ are the polar and azimuthal angles. The unit-vectors in spherical coordinates are denoted by \mathbf{e}_r , \mathbf{e}_θ , and \mathbf{e}_φ . In terms of the incident (in) and scattered (sc) fields, the vector displacements are expressed as

$$\mathbf{u}^{(L)} = \mathbf{u}_{in}^{(L)} + \mathbf{u}_{sc}^{(L)}, \quad (8a)$$

$$\mathbf{u}^{(S)} = \mathbf{u}_{in}^{(S)} + \mathbf{u}_{sc}^{(S)}. \quad (8b)$$

Let us first discuss the solutions of the Helmholtz vector equations in (7) for the incident wave. They should be finite everywhere in space. The regular base solution of the vector Helmholtz equations in spherical coordinates are given in terms of the Hansen vectors⁵⁵ (p. 1799)

$$\mathbf{L}_{nm}^{(1)} = \nabla_L [j_n(k_L r) Y_n^m(\theta, \varphi)] = j_n'(k_L r) \mathbf{Y}_{nm}(\theta, \varphi) + \frac{j_n(k_L r)}{k_L r} \mathbf{\Psi}_{nm}(\theta, \varphi), \quad (9a)$$

$$\mathbf{M}_{nm}^{(1)} = \nabla_S \times [k_S r j_n(k_S r) \mathbf{Y}_{nm}(\theta, \varphi)] = -j_n(k_S r) \mathbf{\Phi}_{nm}(\theta, \varphi), \quad (9b)$$

$$\mathbf{N}_{nm}^{(1)} = \nabla_S \times \mathbf{M}_{nm}^{(1)} = n(n+1) \frac{j_n(k_S r)}{k_S r} \mathbf{Y}_{nm}(\theta, \varphi) + \frac{\partial_r [r j_n(k_S r)]}{k_S r} \mathbf{\Psi}_{nm}(\theta, \varphi), \quad (9c)$$

where $\nabla_j = k_j^{-1} \nabla$ with $j \in \{L, S\}$, j_n is the n th-order spherical Bessel function, the prime symbol means differentiation. The vector spherical harmonics in these equations are defined as⁵⁶

$$\mathbf{Y}_{nm}(\theta, \varphi) \equiv Y_n^m(\theta, \varphi) \mathbf{e}_r, \quad \mathbf{\Psi}_{nm}(\theta, \varphi) \equiv r \nabla Y_n^m(\theta, \varphi), \quad \mathbf{\Phi}_{nm}(\theta, \varphi) \equiv \mathbf{r} \times \nabla Y_n^m(\theta, \varphi). \quad (10)$$

The spherical harmonic of n th-order and m th-degree is

$$Y_n^m(\theta, \varphi) = \sqrt{\frac{(2n+1)(n-m)!}{4\pi(n+m)!}} P_n^m(\cos\theta) e^{im\varphi}, \quad (11)$$

where⁵⁷

$$P_n^m(z) = \frac{(-1)^m}{2^n n!} (1-z^2)^{m/2} \frac{d^{n+m}}{dz^{n+m}} (z^2-1)^n \quad (12)$$

being the associated Legendre polynomial of n th-order and m th-degree.

The partial-wave expansion of the longitudinal and shear displacements are expressed as

$$\mathbf{u}_{\text{in}}^{(\text{L})} = \sum_{n,m} a_{nm}^{(\text{L})} \mathbf{L}_{nm}^{(1)}(k_{\text{L}}r, \theta, \varphi), \quad (13a)$$

$$\mathbf{u}_{\text{in}}^{(\text{S})} = \sum_{n,m} a_{nm}^{(\text{S},1)} \mathbf{M}_{nm}^{(1)}(k_{\text{S}}r, \theta, \varphi) + a_{nm}^{(\text{S},2)} \mathbf{N}_{nm}^{(1)}(k_{\text{S}}r, \theta, \varphi), \quad (13b)$$

where $\sum_{n,m} = \sum_{n=0}^{\infty} \sum_{m=-n}^n$, $a_{nm}^{(\text{L})}$ is the expansion (beam-shape) coefficient of the longitudinal wave, while $a_{nm}^{(\text{S},1)}$ and $a_{nm}^{(\text{S},2)}$ are the expansion coefficients of the of the first- and second-type shear wave. The beam-shape coefficients can be determined by using the orthogonal relations in (A1) into Eqs. (13a) and (13b). The result yields

$$a_{nm}^{(\text{L})} = \frac{1}{j_n'(k_{\text{L}}r)} \oint_{4\pi} \mathbf{u}_{\text{in}}^{(\text{L})}(k_{\text{L}}r, \theta, \varphi) \cdot \mathbf{Y}_{nm}^*(\theta, \varphi) d\Omega, \quad (14a)$$

$$a_{nm}^{(\text{S},1)} = -\frac{1}{n(n+1)j_n(k_{\text{S}}r)} \oint_{4\pi} \mathbf{u}_{\text{in}}^{(\text{S})}(k_{\text{S}}r, \theta, \varphi) \cdot \mathbf{\Phi}_{nm}^*(\theta, \varphi) d\Omega, \quad (14b)$$

$$a_{nm}^{(\text{S},2)} = \frac{k_{\text{S}}r}{n(n+1)j_n(k_{\text{S}}r)} \oint_{4\pi} \mathbf{u}_{\text{in}}^{(\text{S})}(k_{\text{S}}r, \theta, \varphi) \cdot \mathbf{Y}_{nm}^*(\theta, \varphi) d\Omega, \quad (14c)$$

where asterix denotes complex conjugation, the centered dot means scalar product, and $d\Omega = \sin\theta d\theta d\varphi$ is the differential solid angle. We note that the beam-shape coefficients can also be computed by numerical schemes for a given longitudinal or shear incident vector displacements. This is particularly useful in off-axial scattering problems^{58–60}.

The asymptotic form of the incident displacement fields at the farfield ($k_{\text{L}}r, k_{\text{S}}r \rightarrow \infty$) is necessary to derive the extended optical theorem later. Thus, using the asymptotic expression⁵⁷ $j_n(x) = x^{-1} \cos[x - (n+1)\pi/2] + O(x^{-2})$ into (13), we arrive at

$$\mathbf{u}_{\text{in}}^{(\text{L})} = -\frac{1}{k_{\text{L}}r} \sum_{n,m} a_{nm}^{(\text{L})} \sin\left[k_{\text{L}}r - \frac{(n+1)\pi}{2}\right] \mathbf{Y}_{nm}(\theta, \varphi), \quad (15a)$$

$$\begin{aligned} \mathbf{u}_{\text{in}}^{(\text{S})} = & -\frac{1}{k_{\text{S}}r} \sum_{n,m} \left\{ a_{nm}^{(\text{S},1)} \cos\left[k_{\text{S}}r - \frac{(n+1)\pi}{2}\right] \mathbf{\Phi}_{nm}(\theta, \varphi) \right. \\ & \left. + a_{nm}^{(\text{S},2)} \sin\left[k_{\text{S}}r - \frac{(n+1)\pi}{2}\right] \mathbf{\Psi}_{nm}(\theta, \varphi) \right\}. \end{aligned} \quad (15b)$$

We turn our attention to the longitudinal and shear scattered waves. The displacement associated to these waves can also be expanded into partial-waves likewise Eqs. (13a) and (13b). The domain of the scattered displacement fields should excludes the scatterer. In this case, the radial component of the vector spherical functions should satisfy radiation conditions⁶¹. Hence, the regular spherical Bessel functions j_n in the basis vector functions given in (13) should be replaced by the spherical Hankel functions of the first type $h_n^{(1)}$. By so doing, we introduce the singular Hensen vectors

$$\mathbf{L}_{nm}^{(2)} = h_n^{(1)'}(k_{\text{L}}r) \mathbf{Y}_{nm}(\theta, \varphi) + \frac{h_n^{(1)}(k_{\text{L}}r)}{k_{\text{L}}r} \mathbf{\Psi}_{nm}(\theta, \varphi), \quad (16a)$$

$$\mathbf{M}_{nm}^{(2)} = -h_n^{(1)}(k_{\text{S}}r) \mathbf{\Phi}_{nm}(\theta, \varphi), \quad (16b)$$

$$\mathbf{N}_{nm}^{(2)} = n(n+1) \frac{h_n^{(1)}(k_{\text{S}}r)}{k_{\text{S}}r} \mathbf{Y}_{nm}(\theta, \varphi) + \frac{\partial_r[rh_n^{(1)}(k_{\text{S}}r)]}{k_{\text{S}}r} \mathbf{\Psi}_{nm}(\theta, \varphi). \quad (16c)$$

Now, we express the scattering displacements as

$$\mathbf{u}_{\text{sc}}^{(\text{L})}(k_{\text{L}}r, \theta, \varphi) = \sum_{n,m} s_{nm}^{(\text{L})} \mathbf{L}_{nm}^{(2)}(k_{\text{L}}r, \theta, \varphi), \quad (17a)$$

$$\mathbf{u}_{\text{sc}}^{(\text{S})}(k_{\text{S}}r, \theta, \varphi) = \sum_{n,m} s_{nm}^{(\text{S},1)} \mathbf{M}_{nm}^{(2)}(k_{\text{S}}r, \theta, \varphi) + s_{nm}^{(\text{S},2)} \mathbf{N}_{nm}^{(2)}(k_{\text{S}}r, \theta, \varphi), \quad (17b)$$

where $s_{nm}^{(\text{L})}$ is the longitudinal, and $s_{nm}^{(\text{S},1)}$ and $s_{nm}^{(\text{S},2)}$ are the first- and second-type shear scattering coefficients. These coefficients can be determined by applying the continuity condition on the displacement and stress fields across the inclusion's boundary as will be shown later.

Using the asymptotic form of the spherical Hankel function for large arguments⁵⁷ $h_n^{(1)}(x) = (-i)^{n+1}e^{ix}/x + O(x^{-2})$ into Eqs. (17a) and (17b), we obtain the asymptotic behavior of the scattered waves at the farfield,

$$\mathbf{u}_{\text{sc}}^{(j)} = \frac{e^{ik_j r}}{k_j r} \mathbf{f}^{(j)}(\theta, \varphi) + O[(k_j r)^{-2}], \quad j \in \{\text{L}, \text{S}\}. \quad (18)$$

90 The scattering form functions are given by

$$\mathbf{f}^{(\text{L})}(\theta, \varphi) = \sum_{n,m} i^{-n} s_{nm}^{(\text{L})} \mathbf{Y}_{nm}(\theta, \varphi), \quad (19a)$$

$$\mathbf{f}^{(\text{S})}(\theta, \varphi) = \sum_{n,m} i^{-n} [i s_{nm}^{(\text{S},1)} \mathbf{\Phi}_{nm}(\theta, \varphi) + s_{nm}^{(\text{S},2)} \mathbf{\Psi}_{nm}(\theta, \varphi)]. \quad (19b)$$

Using the equations in (A3) and (A4), we derive scattering function in the forward and backward directions as

$$\mathbf{f}^{(\text{L})}(\theta = 0, \pi, \varphi = 0) = \sum_{n=0}^{\infty} \epsilon_n i^n \sqrt{\frac{2n+1}{4\pi}} s_{n,0}^{(\text{L})} \mathbf{e}_z, \quad (20a)$$

$$\begin{aligned} \mathbf{f}^{(\text{S})}(\theta = 0, \pi, \varphi = 0) = & - \sum_{n=1}^{\infty} \frac{\epsilon_n i^n}{2} \sqrt{\frac{(2n+1)n(n+1)}{4\pi}} \left[\left(s_{n,-1}^{(\text{S},1)} + s_{n,1}^{(\text{S},1)} - s_{n,-1}^{(\text{S},2)} + s_{n,1}^{(\text{S},2)} \right) \mathbf{e}_x \right. \\ & \left. - i \left(s_{n,-1}^{(\text{S},1)} - s_{n,1}^{(\text{S},1)} - s_{n,-1}^{(\text{S},2)} - s_{n,1}^{(\text{S},2)} \right) \mathbf{e}_y \right], \end{aligned} \quad (20b)$$

where $\epsilon_n = -1, (-1)^n$ if $\theta = 0, \pi$; and $\mathbf{e}_x, \mathbf{e}_y$, and \mathbf{e}_z are the Cartesian unit-vectors.

Both longitudinal and shear waves might be transmitted into the inclusion. Since the transmission waves
95 should be regular everywhere inside the inclusion, we have

$$\mathbf{u}_{\text{tr}}^{(\text{L})}(k_{\text{L}}r, \theta, \varphi) = \sum_{n,m} t_{nm}^{(\text{L})} \mathbf{L}_{nm}^{(1)}(k_{\text{L}}r, \theta, \varphi), \quad (21a)$$

$$\mathbf{u}_{\text{tr}}^{(\text{S})}(k_{\text{S}}r, \theta, \varphi) = \sum_{n,m} \left[t_{nm}^{(\text{S},1)} \mathbf{M}_{nm}^{(1)}(k_{\text{S}}r, \theta, \varphi) + t_{nm}^{(\text{S},2)} \mathbf{N}_{nm}^{(1)}(k_{\text{S}}r, \theta, \varphi) \right], \quad (21b)$$

where $t_{nm}^{(\text{L})}$ is the longitudinal, and $t_{nm}^{(\text{S},1)}$ and $t_{nm}^{(\text{S},2)}$ are the shear transmission coefficients. They can also be determined by applying the continuity condition of stresses and displacements across the inclusion's surface.

B. Extended optical theorem

Mechanical waves carry energy while propagating. When a wave encounters an inclusion, part of its energy is extinguished due to scattering and absorption within the inclusion. To analyze this phenomenon it is useful to define the absorption σ_{abs} and scattering σ_{sca} cross-section areas as

$$\sigma_{\text{abs,sca}} \equiv \frac{P_{\text{abs,sca}}}{I_0}, \quad (22)$$

where P_{abs} and P_{sca} are the time-averaged absorbed and scattering power, and I_0 is time-averaged characteristic intensity of the incident beam. This means that the total absorption (scattering) power is equal to the incident intensity I_0 projected onto the absorption (scattering) cross-section area. From the conservation of energy principle, the power removed (extinct) from the incident wave is $P_{\text{ext}} = P_{\text{abs}} + P_{\text{sca}}$. Therefore, the extinction cross-section is given by

$$\sigma_{\text{ext}} = \sigma_{\text{abs}} + \sigma_{\text{sca}}. \quad (23)$$

It is useful to introduce the absorption, scattering, and extinction efficiencies as their respectively cross-sections divided by the sphere's cross-sectional area πa^2 ,

$$Q_{\text{abs,sca,ext}} \equiv \frac{\sigma_{\text{abs,sca,ext}}}{\pi a^2}. \quad (24)$$

To obtain the cross-sections, we have to calculate their corresponding time-averaged powers in terms of the incident and scattered fields. This involves the scalar product of two time-harmonic fields. The time-average over the wave period $2\pi/\omega$ of two time-harmonic functions $f_1 e^{-i\omega t}$ and $f_2 e^{-i\omega t}$, with complex amplitudes f_1 and f_2 , is given by

$$\overline{f_1 e^{-i\omega t} f_2 e^{-i\omega t}} = \frac{1}{2} \text{Re}[f_1^* f_2], \quad (25)$$

where 'Re' means the real-part of.

The total absorbed power is tantamount to minus the time-average of the radial total stress projected onto the element velocity $\partial_t \mathbf{u}$ and integrated over a control sphere of radius approaching to infinite,

$$P_{\text{abs}} = - \lim_{r \rightarrow \infty} r^2 \oint_{4\pi} \overline{(\partial_t \mathbf{u} \cdot \boldsymbol{\sigma})} \cdot \mathbf{e}_r \, d\Omega. \quad (26)$$

100 For a time-harmonic displacement, the element velocity is $\partial_t \mathbf{u} = -i\omega \mathbf{u}$. Using the components of the displacement vector in spherical coordinates⁶² along with Eqs. (15a), (15b), and (18), we find

$$u_r \nabla \cdot \mathbf{u}^* = u_r \partial_r u_r^* + O(r^{-3}), \quad (27a)$$

$$\mathbf{u} \cdot (\nabla \mathbf{u} + \nabla \mathbf{u}^T)^* \cdot \mathbf{e}_r = 2u_r \partial_r u_r^* + u_\theta \partial_r u_\theta^* + u_\varphi \partial_r u_\varphi^* + O(r^{-3}). \quad (27b)$$

Therefore, with these expressions and Eq. (25), we obtain the absorbed power as

$$P_{\text{abs}} = -\frac{\rho_0 \omega}{2} \lim_{r \rightarrow \infty} r^2 \text{Re} \oint_{4\pi} i [c_L^2 u_r \partial_r u_r^* + c_S^2 (u_\theta \partial_r u_\theta^* + u_\varphi \partial_r u_\varphi^*)] d\Omega. \quad (28)$$

Referring to the asymptotic representation of the incident and scattered fields given in Eqs. (15a), (15b), and (18), we may re-write Eq. (28) as

$$P_{\text{abs}} = -\frac{\rho_0 \omega u_0^2}{2} \lim_{r \rightarrow \infty} r^2 \text{Re} \oint_{4\pi} i \left[c_L^2 \left(u_{r,\text{in}}^{(L)} \partial_r u_{r,\text{sc}}^{(L)*} + u_{r,\text{sc}}^{(L)} \partial_r u_{r,\text{in}}^{(L)*} + u_{r,\text{sc}}^{(L)} \partial_r u_{r,\text{sc}}^{(L)*} \right) + c_S^2 \left(\mathbf{u}_{\text{sc}}^{(S)} \cdot \partial_r \mathbf{u}_{\text{in}}^{(S)*} + \mathbf{u}_{\text{in}}^{(S)} \cdot \partial_r \mathbf{u}_{\text{sc}}^{(S)*} + \mathbf{u}_{\text{sc}}^{(S)} \cdot \partial_r \mathbf{u}_{\text{sc}}^{(S)*} \right) \right] d\Omega. \quad (29)$$

Importantly, the terms involving only the incident displacement vector \mathbf{u}_{in} do not contribute to the absorbed power. Since they concern to the wave propagation without an inclusion, we left them out in Eq. (29). We recognize in Eq. (29) that terms involving only scattered fields are related to the scattering power

$$P_{\text{sca}} = \frac{\rho_0 u_0^2}{2} \oint_{4\pi} \left[c_L^3 \left| \mathbf{f}^{(L)}(\theta, \varphi) \right|^2 + c_S^3 \left| \mathbf{f}^{(S)}(\theta, \varphi) \right|^2 \right] d\Omega. \quad (30)$$

105 Now, we obtain the absorption, scattering, and extinction cross-sections in terms of the beam-shape and scattering coefficients. Incorporating the expressions given in (B1) into Eq. (29) results

$$\sigma_{\text{abs}}^{(L)} = -\frac{\rho_0 u_0^2 c_L^3}{2I_0} \text{Re} \sum_{n,m} \left(\left| s_{nm}^{(L)} \right|^2 + s_{nm}^{(L)} a_{nm}^{(L)*} \right), \quad (31a)$$

$$\sigma_{\text{abs}}^{(S)} = -\frac{\rho_0 u_0^2 c_S^3}{2I_0} \text{Re} \sum_{n,m} n(n+1) \left(\left| s_{nm}^{(S,1)} \right|^2 + \left| s_{nm}^{(S,2)} \right|^2 + s_{nm}^{(S,1)} a_{nm}^{(S,1)*} + s_{nm}^{(S,2)} a_{nm}^{(S,2)*} \right). \quad (31b)$$

The absorption cross-section is the sum of the longitudinal and shear components,

$$\sigma_{\text{abs}} = \sigma_{\text{abs}}^{(\text{L})} + \sigma_{\text{abs}}^{(\text{S})}. \quad (32)$$

Similarly, substituting the equations in (B1) into Eq. (30), we get the longitudinal and shear scattering cross-section components,

$$\sigma_{\text{sca}}^{(\text{L})} = \frac{\rho_0 u_0^2 c_{\text{L}}^3}{2I_0} \sum_{n,m} \left| s_{nm}^{(\text{L})} \right|^2, \quad (33a)$$

$$\sigma_{\text{sca}}^{(\text{S})} = \frac{\rho_0 u_0^2 c_{\text{S}}^3}{2I_0} \sum_{n,m} n(n+1) \left(\left| s_{nm}^{(\text{S},1)} \right|^2 + \left| s_{nm}^{(\text{S},2)} \right|^2 \right). \quad (33b)$$

The scattering cross-section is then

$$\sigma_{\text{sca}} = \sigma_{\text{sca}}^{(\text{L})} + \sigma_{\text{sca}}^{(\text{S})}. \quad (34)$$

Equations (32) and (34) show that the contribution of longitudinal and shear waves to the absorption and scattering cross-sections are decoupled. Furthermore, the extinction cross-section comes from the combination of these equations as follows

$$\sigma_{\text{ext}} = -\frac{\rho_0 u_0^2}{2I_0} \text{Re} \sum_{n,m} \left[c_{\text{L}}^3 s_{nm}^{(\text{L})} a_{nm}^{(\text{L})*} + n(n+1) c_{\text{S}}^3 \left(s_{nm}^{(\text{S},1)} a_{nm}^{(\text{S},1)*} + s_{nm}^{(\text{S},2)} a_{nm}^{(\text{S},2)*} \right) \right]. \quad (35)$$

This is *the extended optical theorem* for elastic waves involving a spherical inclusion of a rigid, void, elastic, viscoelastic, or layered material. The properties of the inclusion appear in the scattering coefficients $s_{nm}^{(\text{L})}$, $s_{nm}^{(\text{S},1)}$ and $s_{nm}^{(\text{S},2)}$, while the beam characteristics are present in the beam-shape coefficients $a_{nm}^{(\text{L})}$, $a_{nm}^{(\text{S},1)}$, and $a_{nm}^{(\text{S},2)}$. The extinction power of the longitudinal or shear wave can only happen if that component is present in the incident wave. For instance, if the incident wave is a shear wave only then the longitudinal extinction cross-section is zero, $\sigma_{\text{ext}}^{(\text{L})} = 0$. Even though longitudinal scattered waves are present in the medium due to mode conversion. Same thing happens when the incident wave is purely longitudinal, $\sigma_{\text{ext}}^{(\text{S})} = 0$.

115 C. Boundary conditions and coefficient relations

In the scattering by an isotropic solid sphere embedded in an elastic solid matrix, the boundary conditions require the continuity of the displacement vectors and the stress tensor across the sphere's surface $r = a$. On assuming that the inclusion does not have an energy source, the absorption cross-section satisfies $\sigma_{\text{abs}} \geq 0$. This fact will be used to establish the relations that should be satisfied by the scattering coefficients. Let us
120 consider a longitudinal and shear incident wave separately.

1. Longitudinal waves

Longitudinal waves are characterized by the beam-shape coefficient $a_{nm}^{(\text{L})}$. We see from the equations (9), only shear scattered waves of the second-type described by $s_{nm}^{(\text{S},2)}$ can be produced by mode conversion. Defining $s_{nm}^{(\text{L})} = s_n^{(\text{L})} a_{nm}^{(\text{L})}$ and $s_{nm}^{(\text{S},2)} = s_n^{(\text{S},2)} a_{nm}^{(\text{L})}$; while the transmission coefficients are $t_{nm}^{(\text{L})} = t_n^{(\text{L})} a_{nm}^{(\text{L})}$ and $t_{nm}^{(\text{S},2)} = t_n^{(\text{S},2)} a_{nm}^{(\text{L})}$. The four unknown coefficients $s_n^{(\text{L})}$, $s_n^{(\text{S},2)}$, $t_n^{(\text{L})}$, and $t_n^{(\text{S},2)}$ are determined from the following boundary conditions

$$\oint_{4\pi} \begin{bmatrix} (\mathbf{u}_{\text{in}} + \mathbf{u}_{\text{sc}} - \mathbf{u}_{\text{tr}}) \cdot \mathbf{Y}_{nm}^* \\ (\mathbf{u}_{\text{in}} + \mathbf{u}_{\text{sc}} - \mathbf{u}_{\text{tr}}) \cdot \mathbf{\Psi}_{nm}^* \\ \mathbf{e}_r \cdot (\boldsymbol{\sigma}_{\text{in}} + \boldsymbol{\sigma}_{\text{sc}} - \boldsymbol{\sigma}_{\text{tr}}) \cdot \mathbf{Y}_{nm}^* \\ \mathbf{e}_r \cdot (\boldsymbol{\sigma}_{\text{in}} + \boldsymbol{\sigma}_{\text{sc}} - \boldsymbol{\sigma}_{\text{tr}}) \cdot \mathbf{\Psi}_{nm}^* \end{bmatrix} d\Omega = 0. \quad (36)$$

From Eqs. (31a) and (31b), and knowing that $\sigma_{\text{abs}} \geq 0$, we find that the scaled scattering coefficients satisfy

$$\text{Re} \left[s_n^{(\text{L})} \right] + \left| s_n^{(\text{L})} \right|^2 + n(n+1) \left(\frac{c_{\text{S}}}{c_{\text{L}}} \right)^3 \left| s_n^{(\text{S},2)} \right|^2 \leq 0, \quad n = 0, 1, 2, \dots \quad (37)$$

2. Shear waves

Shear waves are described by two beam-shape coefficients, namely, $a_{nm}^{(S,1)}$ and $a_{nm}^{(S,2)}$. Longitudinal waves are produced from shear waves of the second-type through mode conversion. Thus, we rewrite the scattering and transmission coefficients as $s_{nm}^{(S,j)} = s_n^{(S,j)} a_{nm}^{(S,j)}$ ($j = 1, 2$), $s_{nm}^{(L)} = s_n^{(L)} a_{nm}^{(S,2)}$; and $t_{nm}^{(S,j)} = t_n^{(S,j)} a_{nm}^{(S,j)}$ ($j = 1, 2$), $t_{nm}^{(L)} = t_n^{(L)} a_{nm}^{(S,2)}$. We need six conditions to determine the unknown coefficients $s_n^{(L)}$, $t_n^{(L)}$, $s_n^{(S,j)}$ and $t_n^{(S,j)}$, with $j = 1, 2$. Four conditions are already given in Eq. (36), whereas the additional conditions are

$$\oint_{4\pi} \left[\begin{array}{l} (\mathbf{u}_{\text{in}} + \mathbf{u}_{\text{sc}} - \mathbf{u}_{\text{tr}}) \cdot \Phi_{nm}^* \\ \mathbf{e}_r \cdot (\boldsymbol{\sigma}_{\text{in}} + \boldsymbol{\sigma}_{\text{sc}} - \boldsymbol{\sigma}_{\text{tr}}) \cdot \Phi_{nm}^* \end{array} \right] d\Omega = 0. \quad (38)$$

Having that $\sigma_{\text{abs}} \geq 0$ and using Eqs. (31a) and (31b), we obtain the following relations for the scaled scattering coefficients

$$\text{Re} \left[s_n^{(S,1)} + s_n^{(S,2)} \right] + \left| s_n^{(S,1)} \right|^2 + \left| s_n^{(S,2)} \right|^2 + \frac{1}{n(n+1)} \left(\frac{c_L}{c_S} \right)^3 \left| s_n^{(L)} \right|^2 \leq 0, \quad n = 1, 2, 3, \dots \quad (39)$$

The relations in (37) and (39) are a necessary condition to be satisfied by the scaled scattering coefficients.

D. Elastic radiation force

In this section, we use the optical theorem formalism to derive the elastic radiation force exerted by traveling plane waves propagating along the z -axis on a spherical inclusion of radius a . The linear momentum density p carried by a plane wave is related to the time-averaged energy density E_0 through the expression⁶³ (p. 234)

$$E_0 = \begin{cases} pc_L, & \text{longitudinal} \\ pc_S, & \text{shear.} \end{cases} \quad (40)$$

125 Meanwhile the time-averaged force per unit area (radiation pressure) exerted on a nonreflective interface due to linear momentum transfer from the incident wave is also⁶⁴ $pc_{L,S}$. From the energy-momentum relation in Eq. (40), we conclude that the change in the linear momentum of the incident beam in the scattering process is proportional to extinction power $P_{\text{ext}} = P_{\text{abs}} + P_{\text{sca}}$ and thus related to the cross-section $\sigma_{\text{ext}} = \sigma_{\text{abs}} + \sigma_{\text{sca}}$. The linear momentum change corresponding to absorption σ_{abs} cannot be not replaced. In contrast, the
130 part relative to the scattered power returns to the medium. The projected linear momentum of the scattered waves on the forward direction $\theta = 0^\circ$ should be calculated to obtain the elastic radiation force.

As the scattered wave approaches the farfield region $k_L r, k_S r \gg 1$, it resembles a traveling plane wave. Thus, according to Eq. (40), the scattered linear momentum density in an arbitrary direction at the farfield is given by

$$\mathbf{p}_r = \frac{E_0}{c_j r^2} \frac{d\sigma_{\text{sca}}}{d\Omega} \mathbf{e}_r, \quad j \in \{L, S\}, \quad (41)$$

where

$$\frac{d\sigma_{\text{sca}}}{d\Omega} = \frac{\rho_0 u_0^2}{2I_0} \left[c_L^3 \left| \mathbf{f}^{(L)}(\theta, \varphi) \right|^2 + c_S^3 \left| \mathbf{f}^{(S)}(\theta, \varphi) \right|^2 \right] \quad (42)$$

is the differential scattering cross-section, which follows from Eq. (30). Note that the scattering cross-section is $\sigma_{\text{sca}} = r^{-2} \oint_{4\pi} (d\sigma_{\text{sca}}/d\Omega) r^2 d\Omega$. The total linear momentum density along the forward direction is just

$$\oint_{4\pi} (\mathbf{p}_r \cdot \mathbf{e}_z) r^2 d\Omega = \frac{E_0}{c_j} \oint_{4\pi} \cos \theta \frac{d\sigma_{\text{sca}}}{d\Omega} d\Omega. \quad (43)$$

We recognize that the right-hand side of this equation is related to the spatial average of cosine of the polar scattering angle, also known as the asymmetry parameter⁶⁵ (p. 72),

$$\langle \cos \theta \rangle = \frac{1}{\sigma_{\text{sca}}} \oint_{4\pi} \cos \theta \frac{d\sigma_{\text{sca}}}{d\Omega} d\Omega. \quad (44)$$

For symmetric scattering about $\theta = 90^\circ$, the asymmetry parameter is zero, $\langle \cos \theta \rangle = 0$. If the scattering is more prominent in the forward direction ($\theta = 0^\circ$), $\langle \cos \theta \rangle$ is positive. The asymmetry parameter is negative when more scattering occurs toward the backward direction $\theta = 180^\circ$. By using the relation $E_0 = I_0/c_j$ in Eq. (43), the total linear momentum along the axial direction is given by $(I_0/c_j^2)\langle \cos \theta \rangle \sigma_{\text{sca}}$.

Now we can state that the elastic radiation force is given in terms of the linear momentum extracted from the incident wave and that part taken away by the scattered waves in the forward direction ($\theta = 0^\circ$),

$$F_{\text{rad}}^{(j)} = \frac{I_0}{c_j} \sigma_{\text{rad}}, \quad j \in \{\text{L}, \text{S}\} \quad (45)$$

where

$$\sigma_{\text{rad}} = \sigma_{\text{ext}} - \langle \cos \theta \rangle \sigma_{\text{sca}} = \sigma_{\text{abs}} + (1 - \langle \cos \theta \rangle) \sigma_{\text{sca}} \quad (46)$$

is the radiation force cross-section. Thus, the radiation force efficiency reads

$$Q_{\text{rad}} = Q_{\text{abs}} + (1 - \langle \cos \theta \rangle) Q_{\text{sca}}. \quad (47)$$

In terms of this efficiency we have

$$F_{\text{rad}}^{(j)} = \pi a^2 \frac{I_0}{c_j} Q_{\text{rad}}. \quad (48)$$

For a non-absorbing inclusion, the elastic radiation force depends only on the scattering efficiency,

$$F_{\text{rad}}^{(j)} = \pi a^2 \frac{I_0}{c_j} (1 - \langle \cos \theta \rangle) Q_{\text{sca}}. \quad (49)$$

To obtain a useful radiation force formula, we need to calculate $Q_{\text{sca}}\langle \cos \theta \rangle$ in terms of the scattering coefficients. In so doing, we use Eqs. (19a) and (19b) with (A1) and (A6) into Eq. (44). Accordingly, we find

$$\begin{aligned} \langle \cos \theta \rangle Q_{\text{sca}} = & \\ & \frac{\rho_0 u_0^2}{\pi a^2 I_0} \text{Re} \sum_{n,m} \left\{ i \sqrt{\frac{(n+m+1)(n-m+1)}{(2n+3)(2n+1)}} \left[c_{\text{L}}^3 s_{n+1,m}^{(\text{L})*} s_{nm}^{(\text{L})} + c_{\text{S}}^3 n(n+2) \left(s_{n+1,m}^{(\text{S},2)*} s_{nm}^{(\text{S},2)} + s_{n+1,m}^{(\text{S},1)*} s_{nm}^{(\text{S},1)} \right) \right] \right. \\ & \left. + c_{\text{S}}^3 m s_{nm}^{(\text{S},1)} s_{nm}^{(\text{S},2)*} \right\}. \end{aligned} \quad (50)$$

Here, the contribution of the longitudinal and shear scattered waves are decoupled. However, the last term within the curly brackets involves a crossed contribution of both types of shear scattered waves.

Let us examine the direction of the elastic radiation force. Granted that no energy source is inside the inclusion, the absorption efficiency satisfies $Q_{\text{abs}} \geq 0$. Moreover, the scattering efficiency is always positive, $Q_{\text{sca}} > 0$. So, having $|\langle \cos \theta \rangle| < 1$, we conclude that

$$0 < (1 - \langle \cos \theta \rangle) Q_{\text{sca}} < 2Q_{\text{sca}}. \quad (51)$$

Thus, the radiation force efficiency satisfies

$$0 < Q_{\text{rad}} < Q_{\text{sca}} + Q_{\text{ext}}. \quad (52)$$

This implies that the elastic radiation force due to a traveling plane wave always points towards to the forward scattering direction. For a non-dissipative inclusion, we have $0 < Q_{\text{rad}} < 2Q_{\text{sca}}$.

A similar result to Eq. (48) has been earlier obtained for the acoustic radiation force in fluids caused by a plane wave^{66,67} and a Bessel beam⁶⁸. The same expression has also been found for electromagnetic plane waves⁶⁹. This shows a universal character of the radiation force phenomenon.

145 **III. SOME WAVE EXAMPLES**

A. Longitudinal plane wave

Consider an incident longitudinal plane wave (LPW) propagating along the z -axis toward infinity. The corresponding displacement vector is $\mathbf{u}_{\text{in}} = u_0 \mathbf{u}_{\text{in}}^{(\text{L})} e^{-i\omega t}$, with its amplitude being

$$\mathbf{u}_{\text{in}}^{(\text{L})} = -i u_0 \nabla_{\text{L}} e^{ik_{\text{L}} z}. \quad (53)$$

The time-averaged incident intensity is

$$I_0 = -\overline{\partial_t \mathbf{u}_{\text{in}} \cdot \boldsymbol{\sigma} \cdot \mathbf{e}_z}. \quad (54)$$

From Eqs. (1) and (53), we find $\boldsymbol{\sigma} \cdot \mathbf{e}_z = i\omega \rho_0 c_{\text{L}} \mathbf{u}_{\text{in}}$ and $\partial_t \mathbf{u}_{\text{in}} = -i\omega \mathbf{u}_{\text{in}}$. Inserting these expressions into Eq. (54) yields

$$I_0 = \frac{\rho_0 c_{\text{L}} (\omega u_0)^2}{2}. \quad (55)$$

The partial-wave expansion of the incident displacement vector is given by⁷⁰

$$\begin{aligned} \mathbf{u}_{\text{in}}^{(\text{L})} &= -\sum_{n=0}^{\infty} i^{n+1} (2n+1) \nabla_{\text{L}} [j_n(k_{\text{L}} r) P_n(\cos \theta)] \\ &= -\sum_{n=0}^{\infty} i^{n+1} \sqrt{4\pi(2n+1)} \mathbf{L}_{n,0}^{(1)}. \end{aligned} \quad (56)$$

Referring to Eqs. (13a) and (11), the longitudinal beam-shape coefficient reads

$$a_{nm}^{(\text{L})} = -i^{n+1} \sqrt{4\pi(2n+1)} \delta_{m,0}. \quad (57)$$

Because the vector spherical harmonics in the equations of (9) are orthogonal, the longitudinal-to-shear mode conversion in the scattering process only involves the second scattering coefficient $s_{nm}^{(\text{S},2)}$. Thus, the scattered displacement vector is given by

$$\begin{aligned} \mathbf{u}_{\text{sc}} &= -\sum_{n=0}^{\infty} i^{n+1} (2n+1) \left[s_n^{(\text{L})} \nabla_{\text{L}} [h_n^{(1)}(k_{\text{L}} r) P_n(\cos \theta)] + s_n^{(\text{S},2)} \nabla_{\text{S}} \times \nabla_{\text{S}} \times [k_{\text{S}} r h_n^{(1)}(k_{\text{S}} r) P_n(\cos \theta) \mathbf{e}_r] \right] \\ &= \sum_{n=0}^{\infty} s_{n,0}^{(\text{L})} \mathbf{L}_{n,0}^{(2)} + s_{n,0}^{(\text{S},2)} \mathbf{N}_{n,0}^{(2)}. \end{aligned} \quad (58)$$

We readily recognize that the longitudinal and shear scattering coefficients are expressed by

$$\begin{pmatrix} s_{nm}^{(\text{L})} \\ s_{nm}^{(\text{S},2)} \end{pmatrix} = -i^{n+1} \sqrt{4\pi(2n+1)} \delta_{m,0} \begin{pmatrix} s_n^{(\text{L})} \\ s_n^{(\text{S},2)} \end{pmatrix}, \quad (59)$$

where $s_n^{(\text{L})}$ and $s_n^{(\text{S},2)}$ are coefficients given in (C2). We also note that they related by

$$s_n^{(\text{S},2)} = \frac{c_{\text{L}} \det \mathbf{D}_n^{(\text{S})}}{c_{\text{S}} \det \mathbf{D}_n^{(\text{L})}} s_n^{(\text{L})}, \quad (60)$$

where $\mathbf{D}_n^{(\text{L})}$ and $\mathbf{D}_n^{(\text{S})}$ are matrices given in C.

By substituting Eqs. (57) and (59) into Eqs. (31a) and (31b), we obtain the absorbing and scattering efficiencies as

$$Q_{\text{abs}}^{\text{LPW}} = -\frac{4}{x_{\text{L}}^2} \text{Re} \sum_{n=0}^{\infty} (2n+1) \left[s_n^{(\text{L})} + |s_n^{(\text{L})}|^2 + n(n+1) \left(\frac{c_{\text{S}}}{c_{\text{L}}} \right)^3 |s_n^{(\text{S},2)}|^2 \right], \quad (61a)$$

$$Q_{\text{sca}}^{\text{LPW}} = \frac{4}{x_{\text{L}}^2} \sum_{n=0}^{\infty} (2n+1) \left[|s_n^{(\text{L})}|^2 + n(n+1) \left(\frac{c_{\text{S}}}{c_{\text{L}}} \right)^3 |s_n^{(\text{S},2)}|^2 \right], \quad (61b)$$

where $x_L = k_L a$ is the longitudinal sphere size parameter. Note that the shear scattering coefficient $s_n^{(S,2)}$ can be eliminated in the absorption and scattering efficiencies by means of Eq. (60). The scattering cross-section presented here agrees with that previously obtained in Ref.⁷¹. One can verify this by setting $s_n^{(L)} = i^{-n-1} k_L A_n^*/(2n+1)$ and $s_n^{(S,2)} = -i^{-n-1} k_S B_n^*/(2n+1)$, where A_n and B_n are the expansion coefficients in the notation of Ref.⁷¹.

Referring to Eq. (20a), the forward scattering function is given by

$$\mathbf{f}^{(L)}(0,0) = -i \sum_{n=0}^{\infty} (2n+1) s_n^{(L)} \mathbf{e}_z. \quad (62)$$

Hence, using Eq. (35), we find the optical theorem

$$\sigma_{\text{ext}}^{\text{LPW}} = \frac{4\pi}{k_L^2} \text{Im} \left[\mathbf{f}^{(L)}(0,0) \right] \cdot \mathbf{e}_z, \quad (63)$$

where ‘Im’ means the imaginary-part of. This equation states that the extinction cross-section is related to the scattering function along the the forward direction⁶.

Now we are able to calculate the efficiency of the elastic radiation force exerted on the inclusion. The linear momentum taken away from the incident wave is obtained substituting the scattering coefficients given in Eq. (59) into Eq. (50). Finally, using Eqs. (61a) and (61b), we arrive at

$$Q_{\text{rad}}^{\text{LPW}} = -\frac{4}{x_L^2} \text{Re} \sum_{n=0}^{\infty} \left[(2n+1) s_n^{(L)} + 2(n+1) \left\{ s_n^{(L)} s_{n+1}^{(L)*} + n(n+2) \left(\frac{c_S}{c_L} \right)^3 s_n^{(S,2)} s_{n+1}^{(S,2)*} \right\} \right]. \quad (64)$$

As previously noted, the coefficient $s_n^{(S,2)}$ can be eliminated through the relation in Eq. (60). The last term in the curly brackets are due to mode conversion.

B. Shear plane wave

Without loss of generality, we assume that the shear plane wave (SPW) is polarized along the x -axis and propagates on the z -axis toward infinity. Thus, the incident displacement vector reads

$$\mathbf{u}_{\text{in}} = u_0 \mathbf{u}_{\text{in}}^{(S)} = -i u_0 e^{i k_S z} \mathbf{e}_x. \quad (65)$$

Referring to Eq. (54) and noting that $\boldsymbol{\sigma} \cdot \mathbf{e}_z = i \omega \rho_0 c_S \mathbf{u}_{\text{in}}$, we attain the intensity magnitude

$$I_0 = \frac{\rho_0 c_S (\omega u_0)^2}{2}. \quad (66)$$

The partial-wave expansion of the shear plane wave is given by⁷⁰

$$\mathbf{u}_{\text{in}}^{(S)} = \sum_{n=1}^{\infty} i^{n+1} \frac{2n+1}{n(n+1)} \nabla_S \times \left[(i \sin \varphi + \nabla_S \times \cos \varphi) k_S r j_n(k_S r) P_n^1(\cos \theta) \mathbf{e}_r \right]. \quad (67)$$

To obtain the beam-shape coefficients $a_{nm}^{(S,1)}$ and $a_{nm}^{(S,2)}$ we first note that

$$Y_n^{\pm 1}(\theta, \varphi) = \pm \sqrt{\frac{2n+1}{4\pi n(n+1)}} P_n^1(\cos \theta) e^{\pm i \varphi}. \quad (68)$$

Thus,

$$\begin{pmatrix} \sin \varphi \\ -i \cos \varphi \end{pmatrix} P_n^1(\cos \theta) \mathbf{e}_r = \frac{1}{2i} \sqrt{\frac{4\pi n(n+1)}{2n+1}} \begin{pmatrix} \mathbf{Y}_{n,1}(\theta, \varphi) + \mathbf{Y}_{n,-1}(\theta, \varphi) \\ \mathbf{Y}_{n,1}(\theta, \varphi) - \mathbf{Y}_{n,-1}(\theta, \varphi) \end{pmatrix} \quad (69)$$

From Eqs. (13b), (9b), and (9c), we rewrite the expansion in Eq. (67) as

$$\mathbf{u}_{\text{in}}^{(S)} = \sum_{n=1}^{\infty} \frac{i^{n+1}}{2} \sqrt{4\pi \frac{2n+1}{n(n+1)}} \left(\mathbf{M}_{n,1}^{(1)} + \mathbf{M}_{n,-1}^{(1)} + \mathbf{N}_{n,1}^{(1)} - \mathbf{N}_{n,-1}^{(1)} \right). \quad (70)$$

Hence, we find that the beam-shape coefficients be expressed by

$$\begin{pmatrix} a_{nm}^{(S,1)} \\ a_{nm}^{(S,2)} \end{pmatrix} = \frac{i^{n+1}}{2} \delta_{m,\pm 1} \sqrt{4\pi \frac{2n+1}{n(n+1)}} \begin{pmatrix} 1 \\ m \end{pmatrix}. \quad (71)$$

In the scattering process, shear-to-longitudinal mode conversion takes place. However, shear waves described by the vector spherical harmonic Φ_{nm} cannot be converted to a longitudinal wave. Hence, the beam-shape coefficient $a_{nm}^{(S,1)}$ cannot be associated to the longitudinal scattered wave. Consequently, this wave should have $\cos \varphi$ dependence. Thus, we may express the scattered waves as

$$\begin{aligned} \mathbf{u}_{\text{sc}} &= \sum_{n=1}^{\infty} i^{n+1} \frac{2n+1}{n(n+1)} \left[\nabla_{\text{S}} \times \left(i s_n^{(S,1)} \sin \varphi + s_n^{(S,2)} \nabla_{\text{S}} \times \cos \varphi \right) k_{\text{S}} r h_n^{(1)}(k_{\text{S}} r) P_n^1(\cos \theta) \mathbf{e}_r \right. \\ &\quad \left. + s_n^{(L)} \nabla_{\text{L}} \left(\cos \varphi h_n^{(1)}(k_{\text{L}} r) P_n^1(\cos \theta) \right) \right] \\ &= \sum_{n=1}^{\infty} \sum_{m=-1}^1 \left(s_{nm}^{(S,1)} \mathbf{M}_{n,m}^{(2)} + s_{nm}^{(S,2)} \mathbf{N}_{n,m}^{(2)} + s_{nm}^{(L)} \mathbf{L}_{n,m}^{(2)} \right). \end{aligned} \quad (72)$$

The scattering coefficients are given by

$$\begin{pmatrix} s_{nm}^{(S,1)} \\ s_{nm}^{(S,2)} \\ s_{nm}^{(L)} \end{pmatrix} = \frac{i^{n+1}}{2} \delta_{m,\pm 1} \sqrt{4\pi \frac{2n+1}{n(n+1)}} \begin{pmatrix} s_n^{(S,1)} \\ m s_n^{(S,2)} \\ m s_n^{(L)} \end{pmatrix}. \quad (73)$$

where $s_n^{(S,1)}$, $s_n^{(S,2)}$, and $s_n^{(L)}$ are obtained from the boundary conditions across the inclusions' surface. They are given in (C5).

Now we can obtain the efficiencies by substituting the scattering coefficients into Eqs. (31a), (31b), (33a), and (33b), we arrive at

$$Q_{\text{abs}}^{\text{SPW}} = -\frac{2}{x_{\text{S}}^2} \sum_{n=1}^{\infty} (2n+1) \left[\text{Re} \left(s_n^{(S,1)} + s_n^{(S,2)} \right) + \left| s_n^{(S,1)} \right|^2 + \left| s_n^{(S,2)} \right|^2 + \frac{1}{n(n+1)} \left(\frac{c_{\text{L}}}{c_{\text{S}}} \right)^3 \left| s_n^{(L)} \right|^2 \right], \quad (74a)$$

$$Q_{\text{sca}}^{\text{SPW}} = \frac{2}{x_{\text{S}}^2} \sum_{n=1}^{\infty} (2n+1) \left[\left| s_n^{(S,1)} \right|^2 + \left| s_n^{(S,2)} \right|^2 + \frac{1}{n(n+1)} \left(\frac{c_{\text{L}}}{c_{\text{S}}} \right)^3 \left| s_n^{(L)} \right|^2 \right], \quad (74b)$$

where $x_{\text{S}} = k_{\text{S}} a$ is the shear size parameter of the sphere. The scattering efficiency agrees with the result presented in⁷². Inserting the coefficients given in Eq. (73) into Eq. (20b) yields the forward scattering function

$$\mathbf{f}^{(S)}(0,0) = -\frac{i}{2} \sum_{n=1}^{\infty} (2n+1) \left(s_n^{(S,1)} + s_n^{(S,2)} \right) \mathbf{e}_x. \quad (75)$$

Substituting the scattering coefficients given in (73) into Eq. (35), we obtain the optical theorem

$$\sigma_{\text{ext}}^{\text{SPW}} = \frac{4\pi}{k_{\text{S}}^2} \text{Im} \left[\mathbf{f}^{(S)}(0,0) \right] \cdot \mathbf{e}_x. \quad (76)$$

The extinction cross-section depends on the projection of the scattering function onto the polarization direction. This is in agreement with previous derivations⁶.

Finally, we obtain the efficiency of the elastic radiation force by using the scattering coefficients from (73) into Eqs. (46). Accordingly, we find

$$Q_{\text{rad}}^{\text{SPW}} = -\frac{2}{x_{\text{S}}^2} \text{Re} \sum_{n=1}^{\infty} \left[(2n+1) \left(s_n^{(\text{S},1)} + s_n^{(\text{S},2)} \right) + \frac{2}{n+1} \left\{ n(n+2) \left(s_n^{(\text{S},1)} s_{n+1}^{(\text{S},1)*} + s_n^{(\text{S},2)} s_{n+1}^{(\text{S},2)*} \right) + \frac{2n+1}{n} s_n^{(\text{S},1)} s_n^{(\text{S},2)*} + \left(\frac{c_{\text{L}}}{c_{\text{S}}} \right)^3 s_n^{(\text{L})} s_{n+1}^{(\text{L})*} \right\} \right]. \quad (77)$$

The last term in this equation is due to the shear-to-longitudinal mode conversion in the scattering process. The crossing term $s_n^{(\text{S},1)} s_n^{(\text{S},2)*}$ shows that the contribution from the scattered shear waves is not decoupled.

C. Longitudinal focused beam

We assume that an spherically focused transducer produces longitudinal waves that are scattered by the spherical inclusion placed at the transducer focus (on-focus configuration). The transducer has aperture $2b$, radius of curvature r_0 , and half-spread angle $\alpha_0 = \arcsin(b/r_0)$ as depicted in Fig. 2. We consider the transducer in the paraxial approximation, where its aperture is much larger than the wavelength $k_{\text{L}}b \gg 1$. This implies that $k_{\text{L}}r_0 \gg 1$. In a lossless medium, the axial incident pressure yielded by the transducer is given by⁷³

$$p_{\text{in}} = \frac{ip_0 r_0 e^{ik_{\text{L}}z}}{z - r_0} \left(1 - \exp \left[\frac{ik_{\text{L}}b^2}{2} \left(\frac{1}{z} - \frac{1}{r_0} \right) \right] \right), \quad (78)$$

where p_0 is the pressure magnitude at the source. It is useful to normalize the focused pressure by its maximum value at $z = r_0$, i.e. $|p_{\text{in}}(r_0)| = k_{\text{L}}b^2 p_0 / (2r_0)$. One can show that the beam-shape coefficient of the focused beam is given by⁶⁰

$$a_{nm}^{(\text{L})} = -i^n \sqrt{4\pi(2n+1)} \delta_{m,0} g_n, \quad (79)$$

where

$$g_n = \frac{2e^{ik_{\text{L}}r_0}}{(2n+1) \sin^2 \alpha_0} [P_{n+1}(\cos \alpha_0) - P_{n-1}(\cos \alpha_0)] \quad (80)$$

is the diffraction coefficient. The weakly focused limit $r_0 \gg b$ leads to

$$g_n = -e^{ik_{\text{L}}r_0} + \text{O} \left[\left(\frac{b}{r_0} \right)^2 \right], \quad (81)$$

which corresponds to the plane wave limit.

Referring to Eqs. (59), the longitudinal and shear scattering coefficients are expressed by

$$\begin{pmatrix} s_{nm}^{(\text{L})} \\ s_{nm}^{(\text{S})} \end{pmatrix} = -i^n \sqrt{4\pi(2n+1)} \delta_{m,0} g_n \begin{pmatrix} s_n^{(\text{L})} \\ s_n^{(\text{S},2)} \end{pmatrix}. \quad (82)$$

The coefficients $s_n^{(\text{L})}$ and $s_n^{(\text{S},2)}$ are the same as those found in the scattering of a longitudinal plane wave, since the inclusion is isotropic – see the equations in (C2).

After inserting Eq. (82) into Eqs. (31a), (31b), (33a), and (33b), we obtain the absorbing and scattering efficiencies as

$$Q_{\text{abs}}^{\text{FOC}} = -\frac{4}{x_{\text{L}}^2} \text{Re} \sum_{n=0}^{\infty} (2n+1) |g_n|^2 \left[s_n^{(\text{L})} + |s_n^{(\text{L})}|^2 + n(n+1) \left(\frac{c_{\text{S}}}{c_{\text{L}}} \right)^3 |s_n^{(\text{S},2)}|^2 \right], \quad (83a)$$

$$Q_{\text{sca}}^{\text{FOC}} = \frac{4}{x_{\text{L}}^2} \sum_{n=0}^{\infty} (2n+1) |g_n|^2 \left[|s_n^{(\text{L})}|^2 + n(n+1) \left(\frac{c_{\text{S}}}{c_{\text{L}}} \right)^3 |s_n^{(\text{S},2)}|^2 \right]. \quad (83b)$$

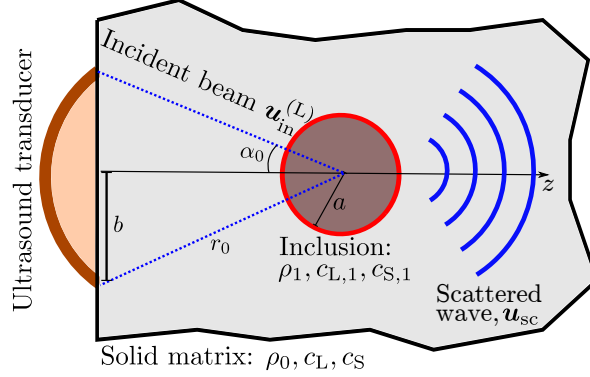


FIG. 2. (Color online) The scattering of a longitudinal focused beam by a sphere of radius a . The incident beam is produced by a spherically focused transducer of aperture $2b$ and half-aperture angle $\alpha_0 = \arcsin(b/r_0)$.

It should be noticed that in the weakly focused regime, $r_0 \gg b$, the scattering efficiency is equal to that of a longitudinal plane wave

$$Q_{\text{sca}}^{\text{FOC}} = Q_{\text{sca}}^{\text{LPW}}. \quad (84)$$

185 The optical theorem for Thus,

$$\begin{aligned} \sigma_{\text{ext}}^{\text{FOC}} &= \frac{4\pi}{k_L^2} \text{Im} \left[-i \sum_{n=0}^{\infty} (2n+1) |g_n|^2 s_n^{(L)} \right] \\ &= \frac{4\pi}{k_L^2} \text{Im} \left[\mathbf{f}^{(L)}(0, 0) \cdot \mathbf{e}_z \right]. \end{aligned} \quad (85)$$

Thus, in the on-focus scattering configuration, the optical theorem has the same format as for a longitudinal plane wave.

We may compute the elastic radiation force exerted on the on-focus sphere totally immersed in the focal region. In such situation, the beam's wavefront can be approached to a traveling plane wave⁷³. Therefore, after inserting Eqs. (83a) and (83b) into Eqs. (48) and (50), we find the axial radiation force efficiency as

$$Q_{\text{rad}}^{\text{FOC}} = -\frac{4}{x_L^2} \text{Re} \sum_{n=0}^{\infty} \left[(2n+1) |g_n|^2 s_n^{(L)} + 2(n+1) g_{n+1}^* g_n \left\{ s_{n+1}^{(L)*} s_n^{(L)} + n(n+2) \left(\frac{c_S}{c_L} \right)^3 s_{n+1}^{(S,2)*} s_n^{(S,2)} \right\} \right]. \quad (86)$$

This efficiency has the same structure of that for a longitudinal plane wave. Though it carries information on diffraction properties of the beam through the g_n -coefficients.

190 IV. NUMERICAL RESULTS

To numerically evaluate the efficiencies which are given by an infinite series, we have to establish a truncation order. Consider that Q_n is the n th-partial term of the efficiencies Q_{sca} and Q_{rad} . Both efficiency series are truncated at the smallest positive integer N to which the condition $|Q_{N+1}| / |\sum_{n=0}^N Q_n| < 10^{-6}$ is satisfied. Furthermore, the scattering coefficients given in C are used to compute Q_{sca} and Q_{rad} .

195 A. Scattering in aluminium matrix

The scattering and elastic radiation force efficiencies are computed for an iron sphere embedded in an aluminum matrix. The physical parameters describing these materials are, respectively, $\rho_1 = 7700 \text{ kg m}^{-3}$, $c_{L,1} = 5790 \text{ m s}^{-1}$, $c_{S,1} = 3100 \text{ m s}^{-1}$; and $\rho_0 = 2700 \text{ kg m}^{-3}$, $c_L = 6568 \text{ m s}^{-1}$, $c_S = 3149 \text{ m s}^{-1}$. As an initial test, we thoroughly reproduced the results presented in Ref.⁷⁴. Also, we numerically obtained the shear

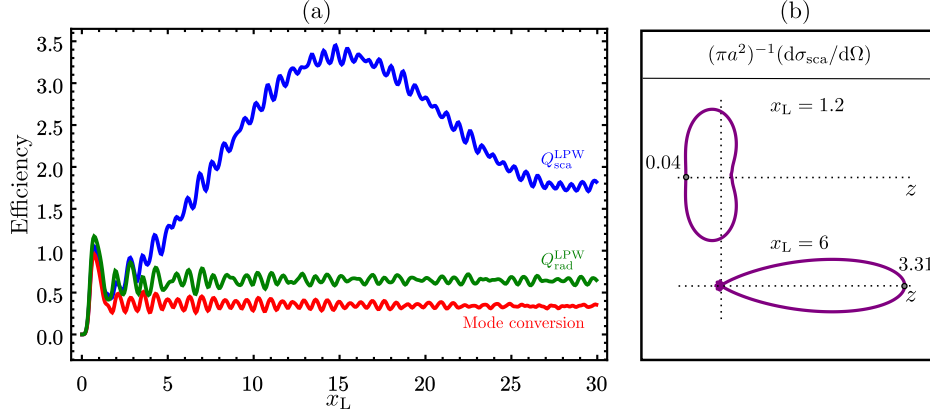


FIG. 3. (Color online) (a) The scattering Q_{sca}^{LPW} and radiation force Q_{rad}^{LPW} efficiencies versus the sphere size factor x_L for a longitudinal plane wave (LPW) scattered by an iron sphere embedded in an aluminum matrix. The mode conversion in scattering is also depicted (red solid line). (b) The normalized differential scattering-cross section computed for $x_L = 1.2$ and $x_L = 6$.

scattering cross-section as given in Ref.¹⁰. In both tests, we found excellent agreement with previous results. For the sake of brevity, we will not show these tests here.

In Fig. 3.a, we show the scattering and radiation force efficiencies of a longitudinal plane wave (LPW). The contribution of mode conversion to Q_{sca} is also depicted. We see that mode conversion is dominant in the band $x_L < 2$. Furthermore, both efficiencies have practically the same magnitude when $x_L < 3$. Rapid fluctuations in the efficiencies, due to resonances⁷⁰, are observed. Around $x_L = 1.2$, we have $Q_{rad}^{LPW} < Q_{sca}^{LPW}$, so according to Eq. (51), the asymmetry factor should be negative, $\langle \cos \theta \rangle < 0$. This is confirmed in Fig. 3.b by noting that scattering is more prominent in the backward direction. When $x_L > 2$, the opposite happens $Q_{rad}^{LPW} > Q_{sca}^{LPW}$ and thus forward scattering dominates. We also observe that the scattering efficiency slowly converges to 2 as x_L increases. This suggests that longitudinal waves follows the extinction paradox, which states that a very large sphere blocks twice its cross-sectional area⁷⁵ (p. 68).

The radiation force and scattering efficiencies of a shear plane wave polarized along the x -axis is plotted in Fig. 4.a. The contribution from mode conversion to the scattering efficiency is illustrated. It is noticed that mode conversion plays a minor role in the current case. Ripples are observed in both efficiencies due to resonances in the sphere. In the band $x_S < 1.2$ we have $Q_{rad}^{SPW} > Q_{sca}^{SPW}$, and thus the asymmetry factor is negative $\langle \cos \theta \rangle < 0$ as discussed in Eq. (51). In Fig. 4.b, we observe that backscattering is dominant at $x_S = 1.1$. The scattering efficient becomes larger than the radiation force efficiency when $x_S > 1.2$. In this case, forward scattering is dominant and $\langle \cos \theta \rangle > 0$ as depicted in Fig. 4.b.

We show the scattering (solid line) and radiation force (dotted line) efficiencies as a function of x_L for a longitudinal focused beam in Fig. 5. The transducer half-aperture angles are $\alpha_0 = 5^\circ, 10^\circ, 15^\circ$. When $\alpha_0 = 5^\circ$, the efficiency approaches that of a longitudinal plane wave. As the beam becomes more focused, the efficiencies decrease. Also, rapid fluctuations due to resonances in the sphere are observed on both efficiencies. As the sphere size parameter x_L increases, the efficiencies become weaker, i.e. less scattering power is expected. It should be remembered that to compute the radiation force efficiency given in Eq. (86), we have assumed that the sphere is placed at the transducer focus, thoroughly inside the focal region. Such hypothesis is necessary because the energy-momentum relation in Eq. (40) is strictly valid within the focal region in which the wavefronts are nearly plane. Since the beam-waist at 3dB-intensity is⁷⁶ (p. 185) $3.20/(k_L \sin \alpha_0)$, it is prudent to use Eq. (86) within the band $x_L < 3.20/\sin \alpha_0 = 37, 18, 12$ for $\alpha_0 = 5^\circ, 10^\circ, 15^\circ$, respectively.

B. Elastic radiation force in tissue-like medium

The importance of elastic radiation force to ultrasound elastography has prompted us to analyze this force in tissue-like medium using the developed theory here. In so doing, we use the descriptive parameters for gel⁷⁷: density $\rho_0 = 1100 \text{ kg m}^{-3}$, longitudinal speed of sound $c_L = 1500 \text{ m s}^{-1}$, shear elasticity modulus

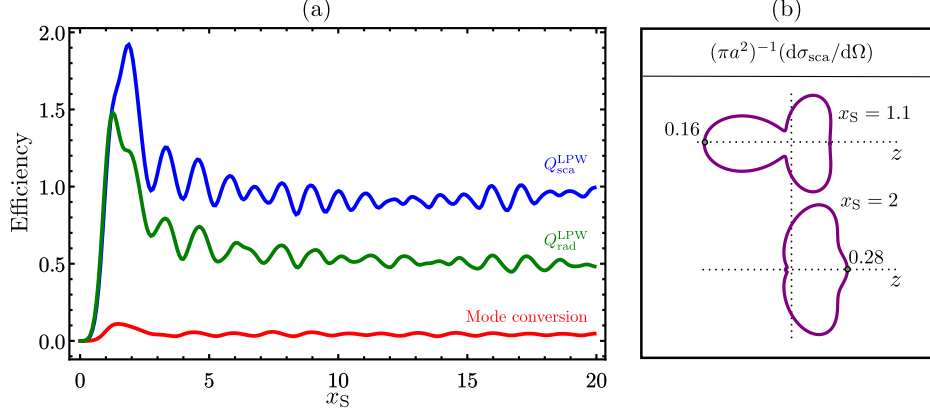


FIG. 4. (Color online)(Color online) (a) The scattering $Q_{\text{sca}}^{\text{SPW}}$ and radiation force $Q_{\text{rad}}^{\text{SPW}}$ efficiencies versus the sphere size factor x_S for a shear plane wave (SPW) scattered by an iron sphere embedded in an aluminum matrix. The mode conversion in scattering is also shown (red solid line). (b) The normalized differential scattering-cross section computed for $x_L = 1.1$ and $x_L = 2$.

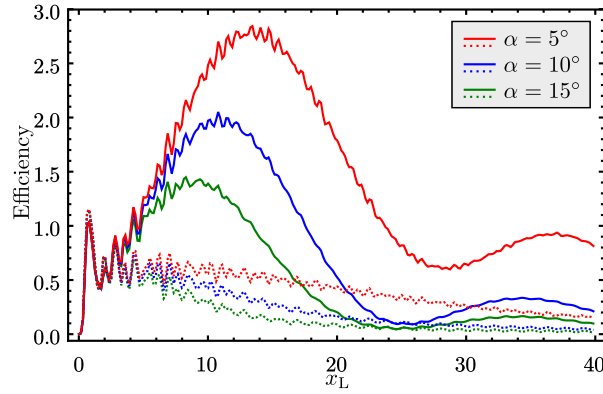


FIG. 5. (Color online) The scattering and radiation force efficiencies (solid and dotted lines, respectively) versus the size factor x_L for a longitudinal focused beam scattered by an iron sphere in an aluminum matrix. The transducer half-aperture angles are $\alpha_0 = 5^\circ, 10^\circ, 15^\circ$.

$\mu_{0,E} = 5360 \text{ Pa}$, and shear viscosity $\mu_{0,V} = 0.36 \text{ Pa} \cdot \text{s}$. The shear speed of sound is calculate through the formula⁷⁸

$$c_S = \sqrt{\frac{2(\mu_{0,E}^2 + \omega^2 \mu_{0,V}^2)}{\rho_0(\mu_{0,E} + \sqrt{\mu_{0,E}^2 + \omega^2 \mu_{0,V}^2})}}. \quad (87)$$

For a typical ultrasound frequency in elastography $\omega/2\pi = 2.25 \text{ MHz}$, we have $c_S = 99.3 \text{ m s}^{-1}$. The target sphere is assumed to be made of stainless steel (type 4310) with the following parameters: density $\rho_1 = 7840 \text{ kg m}^{-3}$, longitudinal and shear speed of sound $c_{L,1} = 5854 \text{ m s}^{-1}$ and $c_{S,1} = 3150 \text{ m s}^{-1}$. Effects of medium absorption are not considered in this analysis. We will compared the results in gel to those in water at room temperature ($\rho_0 = 1000 \text{ kg m}^{-3}$, $c_L = 1500 \text{ m s}^{-1}$, $c_S = 0$).

In Fig. 6, we show the radiation force efficiency for a longitudinal focused beam with $\alpha_0 = 11.45^\circ$ and a longitudinal plane wave versus the sphere size parameter x_L . The frequency is fixed at 2.25 MHz. It is noticeable that the radiation force of the focused beam in water is in excellent agreement to what has been obtained by Chen and Apfel³⁹. In gel, the shear speed of sound corresponds to 6.6% of its longitudinal counterpart. However, a considerable deviation between the efficiencies in gel and water is observed. For both incident waves, the maximum relative difference, adopting the value in gel as the reference, is 98% at $x_L = 0.16$. Thus, the prediction from the lossless liquid and soft solid significantly deviates in the long-

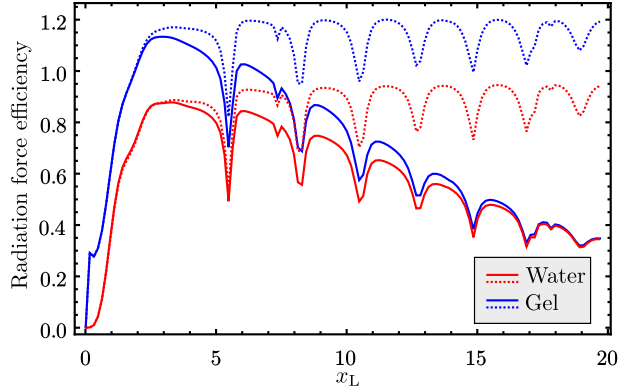


FIG. 6. (Color online) The elastic radiation force efficiency versus the size factor x_L for a longitudinal focused beam (solid lines) and a longitudinal plane wave (dotted lines) scattered by a stainless steel sphere (type 4310) in gel and water. The ultrasound frequency is 2.25MHz and $\alpha_0 = 11.45^\circ$.

wavelength limit $x_L \ll 1$. The relative difference at $x_L = 3.4$ is 23% and still significant. This value remains
 245 the average difference between the plane wave efficiencies.

Some remarks on the radiation force efficiency of the longitudinal focused beam should be drawn. As
 the ratio of the medium sound speeds approaches zero, $c_S/c_L \rightarrow 0$, the efficiency in a soft solid is expected
 to become that in a lossless liquid. We observe that in Fig. 6 by noting that radiation force efficiency in
 water as computed by Chen and Apfel³⁹ is thoroughly recovered. Speculatively, this hints that the radiation
 250 force efficiency in Eq. (86) is valid for any sphere size parameter $x_L > 0$. Holding this view, we notice that
 the difference of the efficiencies in gel and water fades away for $x_L > 14$. Thus, the contribution of mode
 conversion in this band becomes weaker.

V. SUMMARY AND CONCLUSIONS

The extended optical theorem in elastodynamics relates the absorption, scattering, and extinction powers
 255 by expressing them in terms of scattering coefficients. On its turn, these coefficients are computed by solving
 the system of linear equations derived from appropriate continuity conditions of the displacement vectors
 and stress fields across the inclusion's surface. The developed formalism can be applied to the scattering of
 a longitudinal and shear beam with arbitrary wavefront by a spherical inclusion made of any material.

We have revisited the classical problem of plane wave scattering and analyzed the contribution of mode
 260 conversion to the scattered waves. The optical theorem for the scattering of a spherically focused beam by
 an on-focused sphere was established. We have derived for the first time the elastic radiation force exerted
 on a sphere in a solid matrix considering a plane wave and a longitudinal focused beam. The case of an
 iron sphere embedded in an aluminum solid matrix was examined. Additionally, the radiation force on a
 stainless steel sphere embedded in a gel (soft solid) was computed. The relative difference between our model
 265 and previous water-like medium approach can be as high as 98% in the long-wavelength limit. Therefore,
 assuming lossless liquid models to estimate the radiation force in soft solids cannot be taken for granted.

In conclusion, the extended optical theorem can be used as a tool to compute the extinction, absorption
 and scattering powers for arbitrary beams such as Gaussian, Bessel, Airy, etc. Such analysis may foster new
 applications in ultrasonic nondestructive testing and geophysics. Furthermore, the optical theorem provides
 270 an elegant and simple way to obtain the elastic radiation force in solids. We expect that our work will have
 direct applications in the development and enhancement of elastography methods.

ACKNOWLEDGEMENTS

This work was partially supported by CNPq (Brazilian agency), Grant No. 303783/2013-3.

Appendix A: Vector spherical harmonics

275 The vector spherical harmonics (VSH) satisfy the orthogonality relations⁵⁶

$$\oint_{4\pi} \mathbf{Y}_{nm} \cdot \mathbf{Y}_{n_1 m_1}^* d\Omega = \delta_{n, n_1} \delta_{m, m_1}, \quad (\text{A1a})$$

$$\oint_{4\pi} \mathbf{\Psi}_{nm} \cdot \mathbf{\Psi}_{n_1 m_1}^* d\Omega = \oint_{4\pi} \mathbf{\Phi}_{nm} \cdot \mathbf{\Phi}_{n_1 m_1}^* d\Omega = n(n+1) \delta_{n, n_1} \delta_{m, m_1}, \quad (\text{A1b})$$

$$\oint_{4\pi} \mathbf{Y}_{nm} \cdot \mathbf{\Psi}_{n_1 m_1}^* d\Omega = \oint_{4\pi} \mathbf{Y}_{nm} \cdot \mathbf{\Phi}_{n_1 m_1}^* d\Omega = \oint_{4\pi} \mathbf{\Phi}_{nm} \cdot \mathbf{\Psi}_{n_1 m_1}^* d\Omega = 0. \quad (\text{A1c})$$

From VSH definition in (10), we have

$$\mathbf{\Psi}_{nm} = (\partial_\theta Y_n^m) \mathbf{e}_\theta + \frac{1}{\sin \theta} (\partial_\varphi Y_n^m) \mathbf{e}_\varphi, \quad (\text{A2a})$$

$$\mathbf{\Phi}_{nm} = -\frac{1}{\sin \theta} (\partial_\varphi Y_n^m) \mathbf{e}_\theta + (\partial_\theta Y_n^m) \mathbf{e}_\varphi. \quad (\text{A2b})$$

It follows from Eq. (11) and the definition of the associate Legendre functions⁵⁷ that $Y_n^m(0, 0) = \sqrt{(2n+1)/4\pi} \delta_{m,0}$. Thus, the VSH in the forward scattering direction are obtained using this identity and the equations in (A2),

$$\mathbf{Y}_{nm}(0, 0) = \sqrt{\frac{2n+1}{4\pi}} \delta_{m,0} \mathbf{e}_z, \quad (\text{A3a})$$

$$\mathbf{\Psi}_{nm}(0, 0) = \frac{1}{2} \sqrt{\frac{2n+1}{4\pi}} \sqrt{n(n+1)} [(\delta_{m,-1} - \delta_{m,1}) \mathbf{e}_x - i(\delta_{m,-1} + \delta_{m,1}) \mathbf{e}_y], \quad (\text{A3b})$$

$$\mathbf{\Phi}_{nm}(0, 0) = \frac{i}{2} \sqrt{\frac{2n+1}{4\pi}} \sqrt{n(n+1)} [(\delta_{m,-1} + \delta_{m,1}) \mathbf{e}_x - i(\delta_{m,-1} - \delta_{m,1}) \mathbf{e}_y], \quad (\text{A3c})$$

280 where \mathbf{e}_x , \mathbf{e}_y , and \mathbf{e}_z are the Cartesian unit-vectors. Similarly, using the expression $Y_n^m(\pi, 0) = (-1)^n Y_n^m(0, 0)$, we find the VSHs in the backscattering direction $\theta = \pi$,

$$\mathbf{Y}_{nm}(\pi, 0) = (-1)^{n+1} \mathbf{Y}_{nm}(0, 0), \quad (\text{A4a})$$

$$\mathbf{\Psi}_{nm}(\pi, 0) = (-1)^{n+1} \mathbf{\Psi}_{nm}(0, 0), \quad (\text{A4b})$$

$$\mathbf{\Phi}_{nm}(\pi, 0) = (-1)^{n+1} \mathbf{\Phi}_{nm}(0, 0). \quad (\text{A4c})$$

We have used the relations $\mathbf{e}_r(0, 0) = \mathbf{e}_z$, $\mathbf{e}_r(\pi, 0) = -\mathbf{e}_z$, $\mathbf{e}_\theta(0, 0) = \mathbf{e}_x$, $\mathbf{e}_\theta(\pi, 0) = -\mathbf{e}_x$, $\mathbf{e}_\varphi(\pi, 0) = \mathbf{e}_\varphi(0, 0) = \mathbf{e}_y$.

Other common definition of VSH is⁵⁵ (p. 1899)

$$\mathbf{P}_{nm} = (-1)^m \sqrt{\frac{4\pi(n+m)!}{(2n+1)(n-m)!}} \mathbf{Y}_{nm}, \quad (\text{A5a})$$

$$\mathbf{B}_{nm} = \frac{(-1)^m}{\sqrt{n(n+1)}} \sqrt{\frac{4\pi(n+m)!}{(2n+1)(n-m)!}} \mathbf{\Psi}_{nm}, \quad (\text{A5b})$$

$$\mathbf{C}_{nm} = \frac{(-1)^{m+1}}{\sqrt{n(n+1)}} \sqrt{\frac{4\pi(n+m)!}{(2n+1)(n-m)!}} \mathbf{\Phi}_{nm}. \quad (\text{A5c})$$

285 Using the recursion expressions for these vectors given in⁷⁹, we find

$$\cos \theta \mathbf{Y}_{nm} = \sqrt{\frac{(n-m)(n+m)}{(2n-1)(2n+1)}} \mathbf{Y}_{n-1,m} + \sqrt{\frac{(n-m+1)(n+m+1)}{(2n+1)(2n+3)}} \mathbf{Y}_{n+1,m}, \quad (\text{A6a})$$

$$\begin{aligned} \cos \theta \mathbf{\Psi}_{nm} &= \frac{n+1}{n} \sqrt{\frac{(n-m)(n+m)}{(2n-1)(2n+1)}} \mathbf{\Psi}_{n-1,m} + \frac{im}{n(n+1)} \mathbf{\Phi}_{nm} \\ &+ \frac{n}{n+1} \sqrt{\frac{(n-m+1)(n+m+1)}{(2n+1)(2n+3)}} \mathbf{\Psi}_{n+1,m}, \end{aligned} \quad (\text{A6b})$$

$$\begin{aligned} \cos \theta \mathbf{\Phi}_{nm} &= \frac{n+1}{n} \sqrt{\frac{(n-m)(n+m)}{(2n-1)(2n+1)}} \mathbf{\Phi}_{n-1,m} - \frac{im}{n(n+1)} \mathbf{\Psi}_{nm} \\ &+ \frac{n}{n+1} \sqrt{\frac{(n-m+1)(n+m+1)}{(2n+1)(2n+3)}} \mathbf{\Phi}_{n+1,m}. \end{aligned} \quad (\text{A6c})$$

Appendix B: Longitudinal and shear absorption power components

Using Eqs. (15a) and (15b), we find that the terms of the absorbing power given in Eq. (29) at the farfield are

$$\text{Re} \left[i\mathbf{u}_{r,\text{in}}^{(\text{L})} \cdot \partial_r \mathbf{u}_{r,\text{sc}}^{(\text{L})*} + i\mathbf{u}_{r,\text{sc}}^{(\text{L})} \cdot \partial_r \mathbf{u}_{r,\text{in}}^{(\text{L})*} \right] = \frac{1}{k_{\text{L}} r^2} \text{Re} \sum_{\substack{n,m \\ n_1,m_1}} s_{nm}^{(\text{L})} a_{n_1 m_1}^{(\text{L})*} \mathbf{Y}_n^m \mathbf{Y}_{n_1}^{m_1*}, \quad (\text{B1a})$$

$$\text{Re} \left[i\mathbf{u}_{r,\text{sc}}^{(\text{L})} \cdot \partial_r \mathbf{u}_{r,\text{sc}}^{(\text{L})*} \right] = \frac{1}{k_{\text{L}} r^2} \text{Re} \sum_{\substack{n,m \\ n_1,m_1}} s_{nm}^{(\text{L})} s_{n_1 m_1}^{(\text{L})*} \mathbf{Y}_n^m \mathbf{Y}_{n_1}^{m_1*}, \quad (\text{B1b})$$

$$\text{Re} \left[i\mathbf{u}_{\text{sc}}^{(\text{S})} \cdot \partial_r \mathbf{u}_{\text{in}}^{(\text{S})*} + i\mathbf{u}_{\text{in}}^{(\text{S})} \cdot \partial_r \mathbf{u}_{\text{sc}}^{(\text{S})*} \right] = \frac{1}{k_{\text{S}} r^2} \text{Re} \sum_{\substack{n,m \\ n_1,m_1}} \left[s_{nm}^{(\text{S},1)} a_{n_1 m_1}^{(\text{S},1)*} \mathbf{\Phi}_{nm} \cdot \mathbf{\Phi}_{n_1 m_1}^* + s_{nm}^{(\text{S},2)} a_{n_1 m_1}^{(\text{S},2)*} \mathbf{\Psi}_{nm} \cdot \mathbf{\Psi}_{n_1 m_1}^* \right], \quad (\text{B1c})$$

$$\text{Re} \left[i\mathbf{u}_{\text{sc}}^{(\text{S})} \cdot \partial_r \mathbf{u}_{\text{sc}}^{(\text{S})*} \right] = \frac{1}{k_{\text{S}} r^2} \text{Re} \sum_{\substack{n,m \\ n_1,m_1}} \left[s_{n,m}^{(\text{S},1)} s_{n_1,m_1}^{(\text{S},1)*} \mathbf{\Phi}_{nm} \cdot \mathbf{\Phi}_{n_1 m_1}^* + s_{n,m}^{(\text{S},2)} s_{n_1,m_1}^{(\text{S},2)*} \mathbf{\Psi}_{nm} \cdot \mathbf{\Psi}_{n_1 m_1}^* \right]. \quad (\text{B1d})$$

Appendix C: Scattering coefficients

To calculate the longitudinal scattering coefficients we proceed as follows. The incident, scattered, and transmitted displacement vectors are given, respectively, in Eqs. (13), (17), and (21). The corresponding stress tensors are calculated by inserting the displacement vectors into Eq. (1). The obtained displacements and stresses are then substituted in the boundary conditions (36). Hence, we find a system of linear equations for the unknown coefficients,

$$\mathbf{D}_n \mathbf{x}_n^T = \begin{bmatrix} d_{11} & d_{12} & d_{13} & d_{14} \\ d_{21} & d_{22} & d_{23} & d_{24} \\ d_{31} & d_{32} & d_{33} & d_{34} \\ d_{41} & d_{42} & d_{43} & d_{44} \end{bmatrix} \begin{bmatrix} s_n^{(\text{L})} \\ s_n^{(\text{S})} \\ t_n^{(\text{L})} \\ t_n^{(\text{S})} \end{bmatrix} = \begin{bmatrix} b_1 \\ b_2 \\ b_3 \\ b_4 \end{bmatrix} = \mathbf{b}_n^T. \quad (\text{C1})$$

According to the Cramer's rule, the scattering coefficients are given by

$$s_n^{(\text{L})} = \frac{\det \mathbf{D}_n^{(\text{L})}}{\det \mathbf{D}_n}, \quad s_n^{(\text{S})} = \frac{c_{\text{L}} \det \mathbf{D}_n^{(\text{S})}}{c_{\text{S}} \det \mathbf{D}_n}, \quad (\text{C2})$$

290 where the matrices $\mathbf{D}_n^{(L)}$ and $\mathbf{D}_n^{(S)}$ are given in terms of \mathbf{D}_n , except by replacing, respectively, its first and second columns by \mathbf{b}_n^T . The elements of \mathbf{D}_n are given by

$$\begin{aligned}
d_{11} &= x_L h_n^{(1)'}(x_L), \\
d_{12} &= n(n+1)h_n^{(1)}(x_S), \\
d_{13} &= -x_{L,1} j_n'(x_{L,1}), \\
d_{14} &= -n(n+1)j_n(x_{S,1}), \\
d_{21} &= h_n^{(1)}(x_L), \\
d_{22} &= x_S h_n^{(1)'}(x_S) + h_n^{(1)}(x_S), \\
d_{23} &= -j_n(x_{L,1}), \\
d_{24} &= -[x_{S,1} j_n'(x_{S,1}) + j_n(x_{S,1})], \\
d_{31} &= [2n(n+1) - x_S^2]h_n^{(1)}(x_L) - 4x_L h_n^{(1)'}(x_L), \\
d_{32} &= 2n(n+1) [x_S h_n^{(1)'}(x_S) - h_n^{(1)}(x_S)], \\
d_{33} &= -\frac{\rho_1}{\rho_0} \left(\frac{c_{S,1}}{c_S}\right)^2 [[2n(n+1) - x_{S,1}^2]j_n(x_{L,1}) - 4x_{L,1} j_n'(x_{L,1})], \\
d_{34} &= -2\frac{\rho_1}{\rho_0} \left(\frac{c_{S,1}}{c_S}\right)^2 n(n+1)[x_{S,1} j_n'(x_{S,1}) - j_n(x_{S,1})], \\
d_{41} &= x_L h_n^{(1)'}(x_L) - h_n^{(1)}(x_L), \\
d_{42} &= \left[\left(n(n+1) - \frac{x_S^2}{2} - 1 \right) h_n^{(1)}(x_S) - x_S h_n^{(1)'}(x_S) \right], \\
d_{43} &= -\frac{\rho_1}{\rho_0} \left(\frac{c_{S,1}}{c_S}\right)^2 [x_{L,1} j_n'(x_{L,1}) - j_n(x_{L,1})], \\
d_{44} &= -\frac{\rho_1}{\rho_0} \left(\frac{c_{S,1}}{c_S}\right)^2 \left[\left(n(n+1) - \frac{x_{S,1}^2}{2} - 1 \right) j_n(x_{S,1}) - x_{S,1} j_n'(x_{S,1}) \right], \\
b_1 &= -x_L j_n'(x_L), \\
b_2 &= -j_n(x_L), \\
b_3 &= -[2n(n+1) - x_S^2]j_n(x_L) + 4x_L j_n'(x_L), \\
b_4 &= -x_L j_n'(x_L) + j_n(x_L).
\end{aligned} \tag{C3}$$

These elements have also been obtained in Ref.⁷⁰.

Likewise the longitudinal case, the shear scattering coefficients are obtained from the linear system of equations

$$\mathbf{D}_n \mathbf{x}_n^T = \begin{bmatrix} d_{11} & d_{12} & d_{13} & d_{14} & 0 & 0 \\ d_{21} & d_{22} & d_{23} & d_{24} & 0 & 0 \\ d_{31} & d_{32} & d_{33} & d_{34} & 0 & 0 \\ d_{41} & d_{42} & d_{43} & d_{44} & 0 & 0 \\ 0 & 0 & 0 & 0 & d_{55} & d_{56} \\ 0 & 0 & 0 & 0 & d_{65} & d_{66} \end{bmatrix} \begin{bmatrix} s_n^{(L)} \\ s_n^{(S,2)} \\ t_n^{(L)} \\ t_n^{(S,2)} \\ s_n^{(S,1)} \\ t_n^{(S,1)} \end{bmatrix} = \begin{bmatrix} b_1 \\ b_2 \\ b_3 \\ b_4 \\ b_5 \\ b_6 \end{bmatrix} = \mathbf{b}_n^T. \tag{C4}$$

According to the Cramer's rule, the scattering coefficients are given by

$$s_n^{(L)} = \frac{c_S \det \mathbf{D}_n^{(L)}}{c_L \det \mathbf{D}_n}, \quad s_n^{(S,2)} = \frac{\det \mathbf{D}_n^{(S,2)}}{\det \mathbf{D}_n}, \quad s_n^{(S,1)} = \frac{\det \mathbf{D}_n^{(S,1)}}{\det \mathbf{D}_n}. \tag{C5}$$

Here the matrices $\mathbf{D}_n^{(L)}$, $\mathbf{D}_n^{(S,1)}$, and $\mathbf{D}_n^{(S,2)}$ are obtained from \mathbf{D}_n by, respectively, replacing its first, second,

and third columns by \mathbf{b}_n^T . The additional matrix elements required to compute the scattering coefficients are

$$\begin{aligned}
 d_{55} &= x_S h_n^{(1)}(x_S), \\
 d_{56} &= -x_S j_n(x_{S,1}) \\
 d_{65} &= x_S h_n^{(1)'}(x_S) - h_n^{(1)}(x_S), \\
 d_{66} &= -\frac{\rho_1}{\rho_0} \left(\frac{c_{S,1}}{c_S} \right) \left[x_{S,1} j_n'(x_{S,1}) - j_n(x_{S,1}) \right], \\
 b_1 &= -n(n+1)j_n(x_S), \\
 b_2 &= -[x_S j_n'(x_S) + j_n(x_S)], \\
 b_3 &= -2n(n+1)[x_S j_n'(x_S) - j_n(x_S)], \\
 b_4 &= -\left[\left(n(n+1) - \frac{x_S^2}{2} - 1 \right) j_n(x_S) - x_S j_n'(x_S) \right], \\
 b_5 &= -x_S j_n(x_S), \\
 b_6 &= -[x_S j_n'(x_S) - j_n(x_S)].
 \end{aligned} \tag{C6}$$

- 295 ¹R. G. Newton, Optical theorem and beyond, *Am. J. Phys.* 44 (7) (1976) 639–642.
- ²G. Mie, Beiträge zur Optik trüber Medien, speziell kolloidaler Metallösungen, *Ann. Phys.* 330 (3) (1908) 377–445, in German. doi:10.1002/andp.19083300302.
- ³E. Feenberg, The scattering of slow electrons by neutral atoms, *Phys. Rev.* 40 (1) (1932) 40–54. doi:10.1103/PhysRev.40.40.
- 300 ⁴H. C. van de Hulst, On the attenuation of plane waves by obstacles of arbitrary size and form, *Physica* 15 (8-9) (1949) 740–746. doi:10.1016/0031-8914(49)90079-8.
- ⁵A. T. de Hoop, On the plane-wave extinction cross-section of an obstacle, *Appl. Sci. Res. Sect. B* 7 (1) (1959) 463–469. doi:10.1007/BF02921932.
- ⁶P. J. Barratt, W. D. Collins, The scattering cross-section of an obstacle in an elastic solid for plane harmonic waves, *Math. Proc. Cambridge Philos. Soc.* 61 (04) (1965) 969–981. doi:10.1017/S0305004100039360.
- 305 ⁷J. E. Gubernatis, E. Domany, J. A. Krumhansl, Formal aspects of the theory of the scattering of ultrasound by flaws in elastic materials, *J. Appl. Phys.* 48 (7) (1977) 2804–2811. doi:10.1063/1.324141.
- ⁸V. Varatharajulu, Reciprocity relations and forward amplitude theorems for elastic waves, *J. Math. Phys.* 18 (4) (1977) 537. doi:10.1063/1.523335.
- ⁹V. A. Korneev, L. R. Johnson, Scattering of elastic waves by a spherical inclusion—I. Theory and numerical results, *Geophys. J. Int.* 115 (1993) 230–250.
- 310 ¹⁰V. A. Korneev, L. R. Johnson, Scattering of P and S waves by a spherically symmetric inclusion, *Pure Appl. Geophys.* 147 (1996) 675–718.
- ¹¹R. Glauber, V. Schomaker, The theory of electron diffraction, *Phys. Rev.* 89 (4) (1953) 667–671. doi:10.1103/PhysRev.89.667.
- ¹²G. Dassios, Second order low-frequency scattering by the soft ellipsoid, *SIAM J. Appl. Math.* 38 (3) (1980) 373–381. doi:10.1137/0138031.
- 315 ¹³P. L. Marston, Generalized optical theorem for scatterers having inversion symmetry: Applications to acoustic backscattering, *J. Acoust. Soc. Am.* 109 (4) (2001) 1291–1295. doi:10.1121/1.1352082.
- ¹⁴P. Ratilal, N. C. Makris, Extinction theorem for object scattering in a stratified medium, *J. Acoust. Soc. Am.* 110 (6) (2001) 2924. doi:10.1121/1.1405522.
- 320 ¹⁵G. Kriegsmann, A. Norris, E. Reiss, An optical theorem for acoustic scattering by baffled flexible surfaces, *J. Sound Vib.* 99 (3) (1985) 301–307. doi:10.1016/0022-460X(85)90369-4.
- ¹⁶D. Halliday, A. Curtis, Generalized optical theorem for surface waves and layered media, *Phys. Rev. E* 79 (5) (2009) 056603. doi:10.1103/PhysRevE.79.056603.
- ¹⁷V. A. Markel, L. S. Muratov, M. I. Stockman, T. F. George, Theory and numerical simulation of optical properties of fractal clusters, *Phys. Rev. B* 43 (10) (1991) 8183–8195. doi:10.1103/PhysRevB.43.8183.
- 325 ¹⁸J. A. Lock, J. T. Hodges, G. Gouesbet, Failure of the optical theorem for Gaussian-beam scattering by a spherical particle, *J. Opt. Soc. Am. A* 12 (12) (1995) 2708. doi:10.1364/JOSAA.12.002708.
- ¹⁹G. Gouesbet, On the optical theorem and non-plane-wave scattering in quantum mechanics, *J. Math. Phys.* 50 (11) (2009) 112302. doi:10.1063/1.3256127.
- 330 ²⁰L. Zhang, P. L. Marston, Optical theorem for acoustic non-diffracting beams and application to radiation force and torque, *Biomed. Opt. Express* 4 (9) (2013) 1610–1617.
- ²¹F. G. Mitri, G. T. Silva, Generalization of the extended optical theorem for scalar arbitrary-shape acoustical beams in spherical coordinates, *Phys. Rev. E* 90 (5) (2014) 053204. doi:10.1103/PhysRevE.90.053204.
- ²²G. Gouesbet, Asymptotic quantum inelastic generalized Lorenz-Mie theory, *Opt. Commun.* 278 (1) (2007) 215–220. doi:10.1016/j.optcom.2007.06.006.
- 335 ²³F. G. Mitri, Optical theorem for two-dimensional (2D) scalar monochromatic acoustical beams in cylindrical coordinates., *Ultrasonics* 62 (2015) 20–26. doi:10.1016/j.ultras.2015.02.019.
- ²⁴F. G. Mitri, Extended optical theorem for scalar monochromatic acoustical beams of arbitrary wavefront in cylindrical coordinates., *Ultrasonics* 67 (2016) 129–135. doi:10.1016/j.ultras.2016.01.006.
- 340 ²⁵F. G. Mitri, Generalization of the optical theorem for monochromatic electromagnetic beams of arbitrary wavefront in cylindrical coordinates, *J. Quant. Spectrosc. Radiat. Transf.* 166 (2015) 81–92. doi:10.1016/j.jqsrt.2015.07.016.

- ²⁶R. de L. Kronig, On the theory of dispersion of x-rays, *J. Opt. Soc. Am.* 12 (6) (1926) 547–557. doi:10.1364/JOSA.12.000547.
- ²⁷J. S. Toll, Causality and the dispersion relation: Logical foundations, *Phys. Rev.* 104 (6) (1956) 1760–1770. doi:10.1103/PhysRev.104.1760.
- ²⁸R. G. Newton, Determination of the amplitude from the differential cross section by unitarity, *J. Math. Phys.* 9 (12) (1968) 2050–2055. doi:10.1063/1.1664543.
- ²⁹E. Kraut, Review of theories of scattering of elastic waves by cracks, *IEEE Trans. Sonics Ultrason.* 23 (3) (1976) 162–167. doi:10.1109/T-SU.1976.30856.
- ³⁰M. Kitahara and K. Nakagawa, Elastodynamic optical theorem for the evaluation of scattering cross-sections for a crack, in: D. O. Thompson, D. E. Chimenti (Eds.), *Rev. Prog. Quant. Nondestruct. Eval.*, Springer US, Boston, MA, 1997, pp. 27–34. doi:10.1007/978-1-4615-5947-4.
- ³¹P. S. Carney, E. Wolf, G. S. Agarwal, Diffraction tomography using power extinction measurements, *J. Opt. Soc. Am. A* 16 (11) (1999) 2643–2648.
- ³²J. Groenenboom, R. Snieder, Attenuation, dispersion, and anisotropy by multiple scattering of transmitted waves through distributions of scatterers, *J. Acoust. Soc. Am.* 98 (6) (1995) 3482. doi:10.1121/1.413780.
- ³³L. Margerin, H. Sato, Generalized optical theorems for the reconstruction of Green's function of an inhomogeneous elastic medium, *J. Acoust. Soc. Am.* 130 (6) (2011) 3674–3690. doi:10.1121/1.3652856.
- ³⁴K. Wapenaar, E. Slob, R. Snieder, On seismic interferometry, the generalized optical theorem, and the scattering matrix of a point scatterer, *Geophysics* 75 (3) (2010) SA27–SA35.
- ³⁵A. Maurel, V. Pagneux, F. Barra, F. Lund, Interaction between an elastic wave and a single pinned dislocation, *Phys. Rev. B* 72 (2008) 174110.
- ³⁶J. Krautkramer, H. Krautkramer, *Ultrasonic Testing of Materials*, Springer-Verlag, Berlin, Germany, 1990.
- ³⁷V. P. Smyshlyayev, J. R. Willis, Linear and nonlinear scattering of elastic waves by microcracks, *J. Mech. Phys. Solids* 42 (4) (1994) 585–610.
- ³⁸T. Hasegawa, K. Yosioka, Acoustic radiation force on a solid elastic sphere, *J. Acoust. Soc. Am.* 46 (1969) 1139–1143.
- ³⁹X. Chen, R. E. Apfel, Radiation force on a spherical object in an axisymmetric wave field and its application to the calibration of high-frequency transducers, *J. Acoust. Soc. Am.* 99 (1996) 713–724.
- ⁴⁰P. L. Marston, Axial radiation force of a Bessel beam on a sphere and direction reversal of the force, *J. Acoust. Soc. Am.* 120 (2006) 3518–3524.
- ⁴¹F. G. Mitri, Negative axial radiation force on a fluid and elastic spheres illuminated by a high-order Bessel beam of progressive waves, *J. Phys. A* 42 (2009) 245202.
- ⁴²G. T. Silva, An expression for the radiation force exerted by an acoustic beam with arbitrary wavefront (L), *J. Acoust. Soc. Am.* 130 (2011) 3541–3544.
- ⁴³M. Azarpeyvand, Acoustic radiation force of a Bessel beam on a porous sphere, *J. Acoust. Soc. Am.* 131 (2012) 4337–4348.
- ⁴⁴O. A. Sapozhnikov, M. R. Bailey, Radiation force of an arbitrary acoustic beam on an elastic sphere in a fluid, *J. Acoust. Soc. Am.* 133 (2013) 661–676.
- ⁴⁵D. Baresch, J. L. Thomas, R. Marchiano, Three-dimensional acoustic radiation force on an arbitrarily located elastic sphere, *J. Acoust. Soc. Am.* 133 (2013) 25–36.
- ⁴⁶P. N. T. Wells, H.-D. Liang, Medical ultrasound: imaging of soft tissue strain and elasticity, *J. R. Soc. Interface* doi:10.1098/rsif.2011.0054.
- ⁴⁷A. Sarvazyan, T. J. Hall, M. W. Urban, M. Fatemi, S. R. Aglyamov, B. S. Garra, An overview of elastography – an emerging branch of medical imaging, *Curr. Med. Imaging Rev.* 7 (2011) 255–282.
- ⁴⁸M. L. Palmeri, K. R. Nightingale, Acoustic radiation force-based elasticity imaging methods, *Interface Focus* 6 (2011) 553–564.
- ⁴⁹J. Bercoff, M. Tanter, M. Fink, Supersonic shear imaging: a new technique for soft tissue elasticity mapping, *IEEE Trans. Ultrason. Ferroelectr. Freq. Contr.* 51 (2004) 396–409.
- ⁵⁰O. Ordeig, S. Y. Chin, S. Kim, P. V. Chitnis, S. K. Sia, An implantable compound-releasing capsule triggered on demand by ultrasound, *Sci. Rep.* 6 (22803) (2016) 1–11.
- ⁵¹S. R. Aglyamov, A. B. Karpouk, Y. A. Ilinskii, E. A. Zabolotskaya, S. Y. Emelianov, Motion of a solid sphere in a viscoelastic medium in response to applied acoustic radiation force: Theoretical analysis and experimental verification, *J. Acoust. Soc. Am.* 122 (2007) 1927–1936.
- ⁵²V. G. Andreev, I. Y. Demin, Z. A. Korolkov, A. V. Shanin, Motion of spherical microparticles in a viscoelastic medium under the action of acoustic radiation force, *Bull. Russ. Acad. Sci. Phys.* 80 (2016) 1191–1196.
- ⁵³Y. C. Fung, P. Tong, *Classical and Computational Solid Mechanics*, World Scientific, Singapore, 2001.
- ⁵⁴P. M. Morse, H. Feshbach, *Methods of Theoretical Physics, Part I*, McGraw-Hill Inc., New York, NY USA, 1953.
- ⁵⁵P. M. Morse, H. Feshbach, *Methods of Theoretical Physics, Part II*, McGraw-Hill, Inc., New York, NY USA, 1953.
- ⁵⁶R. G. Barrera, G. A. Estevez, J. Giraldo, Vector spherical harmonics and their application to magnetostatics, *Eur. J. Phys.* 6 (4) (1985) 287–294. doi:10.1088/0143-0807/6/4/014.
- ⁵⁷M. Abramowitz, I. Stegun, *Handbook of Mathematical Functions with Formulas, Graphs, and Mathematical Tables*, Dover Publications, Inc., Mineola, NY, 1964.
- ⁵⁸G. T. Silva, Off-axis scattering of an ultrasound Bessel beam by a sphere, *IEEE Trans. Ultrason. Ferroelectr. Freq. Control* 58 (2011) 298–304.
- ⁵⁹F. G. Mitri, G. T. Silva, Off-axial acoustic scattering of a high-order Bessel vortex beam by a rigid sphere, *Wave Motion* 48 (2011) 392–400.
- ⁶⁰G. T. Silva, A. L. Baggio, J. H. Lopes, F. G. Mitri, Computing the acoustic radiation force exerted on a sphere using the translational addition theorem, *IEEE Trans. Ultrason. Ferroelectr. Freq. Control* 62 (2015) 576–583.
- ⁶¹Y.-H. Pao, V. Varatharajulu, Huygens' principle, radiation conditions, and integral formulas for the scattering of elastic waves, *J. Acoust. Soc. Am.* 59 (6) (1976) 1361–1371. doi:10.1121/1.381022.
- ⁶²K. F. Graff, *Wave Motion in Elastic Solids*, Dover Publications, Inc., Mineola, NY USA, 1991.
- ⁶³W. C. Elmore, M. A. Heald, *Physics of Waves*, Dover Publications, Inc., Mineola, NY USA, 1985.

- 410 ⁶⁴G. R. Torr, The acoustic radiation force, *Am. J. Phys.* 52 (1984) 402–408.
- ⁶⁵C. F. Bohren, D. R. Huffman, *Absorption and Scattering of Light by Small Particles*, John Wiley & Sons, Inc., New York NY, USA, 1998.
- ⁶⁶P. J. Westervelt, The theory of steady forces caused by sound waves, *J. Acoust. Soc. Am.* 23 (1951) 312–315.
- ⁶⁷H. Olsen, W. Romberg, H. Wergeland, Radiation force on bodies in a sound field, *J. Acoust. Soc. Am.* 30 (1) (1958) 69–76.
- 415 ⁶⁸L. Zhang, P. L. Marston, Geometrical interpretation of negative radiation forces of acoustical Bessel beams on spheres, *Phys. Rev. E* 84 (3 Pt 2) (2011) 035601. doi:10.1103/PhysRevE.84.035601.
- ⁶⁹H. C. van de Hulst, *Light Scattering by Small Particles*, Dover Publications, Inc., New York, NY, 1981.
- ⁷⁰D. Brill, G. Gaunaurd, Resonance theory of elastic waves ultrasonically scattered from an elastic sphere, *J. Acoust. Soc. Am.* 81 (1987) 1–21.
- 420 ⁷¹C. F. Ying, R. Truell, Scattering of a plane longitudinal wave by a spherical obstacle in an isotropically elastic solid, *J. Appl. Phys.* 27 (9) (1956) 1086–1097. doi:10.1063/1.1722545.
- ⁷²N. G. Einspruch, E. J. Witterholt, R. Truell, Scattering of a plane transverse wave by a spherical obstacle in an elastic medium, *J. Appl. Phys.* 31 (5) (1960) 806–818. doi:10.1063/1.1735701.
- ⁷³B. G. Lucas, T. G. Muir, The field of a focusing source, *J. Acoust. Soc. Am.* 72 (1982) 1289–1296.
- 425 ⁷⁴L. Flax, H. Überall, Resonant scattering of elastic waves from spherical solid inclusions, *J. Acoust. Soc. Am.* 67 (1980) 1432–1442.
- ⁷⁵R. G. Newton, *Scattering theory of waves and particles*, Springer-Verlag, New York, USA, 1982.
- ⁷⁶G. S. Kino, *Acoustic Waves*, Prentice Hall, Englewood Cliffs, NJ, 1987.
- ⁷⁷S. Chen, M. Fatemi, J. F. Greenleaf, Quantifying elasticity and viscosity from measurement of shear wave speed dispersion, *J. Acoust. Soc. Am.* 115 (2004) 2781–2785.
- 430 ⁷⁸Y. Yamakoshi, J. Sato, T. Sato, Ultrasonic imaging of internal vibration of soft tissue under forced vibration, *IEEE Trans. Ultrason. Ferroelect. Freq. Control* 37 (1990) 45–53.
- ⁷⁹R. E. Clapp, Six integral theorems for vector spherical harmonics, *J. Math. Phys.* 11 (1970) 4–9. doi:10.1063/1.1665069.